Journal of Mathematical Biology manuscript No.
(will be inserted by the editor)

Arthur D. Lander · Qing Nie · Frederic Y.M. Wan · Jian-Jun Xu

Diffusion and Morphogen Gradient Formation – Part I: Extracellular Formulation

the date of receipt and acceptance should be inserted later –

Abstract. Gradients of morphogen concentration are known to be responsible for tissue pattering and the diffusion has been considered the main mechanism for morphogen transport and gradient formation. Recently, some theoreticians and experimentalists have argued that diffusion is not an appropriate transport mechanism and other mechanisms were suggested as replacements. The observations against diffusive transport have been summarized and addressed in [8] on the ba-

Arthur D. Lander: Department of Developmental and Cell Biology and Developmental Biology Center, Univ. of California, Irvine, CA 92697

Qing Nie: Department of Mathematics and Center for Biomedical Engineering, Univ. of California, Irvine, CA 92697

Frederic Y.M. Wan: Department of Mathematics, Univ. of California, Irvine, CA 92697

Jian-Jun Xu: Department of Mathematics, Simon Fraser University, Canada, V5A 1S6

Correspondence to: Qing Nie (qnie@math.uci.edu)

The authors acknowledge Patrick Guidotti, Yuan Lou and J. Lawrence Marsh for useful discussions, the supports from NIH grants R01GM67247 and P20GM066051, and the support of NSF SCREM grant DMS0112416.

Key words: Morphogen Gradient - Ligand Receptor - Reaction Diffusion

sis of results from a quantitative analysis of appropriate mathematical models for the various morphogen activities. It was concluded there that diffusive models of morphogen transport can account for much of the data obtained on biological systems including those that have been used to argue against diffusive transport. When observations and data are correctly interpreted, they not only fail to rule out diffusive transport, they favor it. The mathematical underpinnings of the case for diffusive transport of morphogens presented in [8] are provided in a two-part paper consisting of the present article (Part I) on the morphogen activities in the extracellular space and a sequel (Part II) concerning the effects of endocytosis and receptor synthesis in the intracellular compartments. A principal result of Part II is to reduce the boundary value problem for determining the steady state behavior of the more complete model in the second part (designated as System C in [8]) to the same mathematical problem governing the steady state behavior in the simpler formulation of Part I (designated as System B in [8]). The eigenvalue problem in the linear stability analysis of System C is also reduced to the corresponding problem for the simpler System B except for the decay time determined by the smallest root of a different polynomial. Hence, it is adequate and preferable to work with a formulation without internalization for research on the steady state effects of other morphogen activities such as Dpp binding with the HSPG family of non-receptors.

1. Introduction

Classes of molecules, collectively referred to as *morphogens*, are known to be responsible for the patterning of biological tissues. The locations of structures and cell types in an embryo are typically specified by the concentration gradients of different morphogens (that are bound to cell receptors)

during the developmental phase of the biological organism. In many cases, it is well established that a bound morphogen complex concentration gradient is formed by morphogens transported from a localized production site and bound to available cell surface receptor downstream. This can be seen from an in vivo visualization of the gradient of the morphogen Dpp in a Drosophila (fruit fly) wing imaginal disc (Figure 2 of [2]). Figure 1 of [5] indicates the evolution of the morphogen gradient in a wing disc leading to a specific pattern of veins. (Additional evidence and references can be found in [8].) In the past, conventional wisdom was that diffusion would be the main mechanism for transporting morphogens away from production site leading to gradient formation. Recently, some theoreticians and experimentalists have argued that diffusion is not an appropriate transport mechanism and other mechanisms have been suggested instead.

On the theoretical side, Kerszberg and Wolpert [7] simulated the random movement of morphogen molecules over 180 cells. If capture by cell surface receptors is efficient, a specie of morphogen would saturate all receptors in a region of tissue before being able to diffuse further. In that case, no bound morphogen concentration gradient could ever be formed; instead a "wave" of complete receptor activation should move out over time from the morphogen source. On the other hand, in order for diffusion to be an effective transport mechanism, the concentration of surface receptors would have to be so low that the resulting bound morphogen gradient would not

be biologically useful. Hence, some mechanism other than free diffusion must be found for morphogen gradient formation.

Advances in experimental techniques have also led to argument for other transport mechanisms. Fusing Dpp to green fluorescent protein (Dpp-GFP) in the Drosophila wing disc has made it possible to visualize morphogen gradient in vivo and to study its response to experimental manipulation [2] [22]. Some of the observations from such experiments have been interpreted as evidence against diffusive morphogen transport. These include a substantial amount of bound Dpp in gradient system being located inside cells [2] [3] [21] [22] and inhibition of endocytosis disrupting the morphogen gradient and its patterning effects to result in a decrease in overall levels of Dpp-GFP in the morphogen field [2] [4]. These observations and others summarized in [8] have been viewed as evidence in support of a transcytotic mechanism of morphogen transport.

In view of the conflicting intuitive interpretations of available data and developments, it would be desirable to have an analytical basis for settling the current uncertainty regarding the morphogen transport mechanism. References to previous quantitative studies of morphogens and signaling can be found in monographs such as [11] [14]. These studies were generally concerned with other aspects of morphogenesis as were more recent publications in the mathematical biology literature such as [13] [12] [15] [16] [17]. To deal directly with the issue of diffusion as a mechanism for transport of morphogens such as Dpp and the formation of receptor activation gradi-

ents of sufficient duration to stimulate signaling, we have developed a series of mathematical models of different levels of complexity that account for the various interacting morphogen dynamics such as diffusion, reversible binding to receptors, non-receptors (e.g., those of the HSPG family) and other molecules (co-receptors such as Sog), dissociation, degradation, internalization (endocytosis and exocytosis), etc. We have succeeded in extracting useful information about bound Dpp gradients from these models by mathematical analysis and computational methods, making use of available experimental data for input parameter values.

The first group of results from this project were summarized in [8] to address the observations and arguments against diffusive transport. It was concluded there that diffusive models of morphogen transport can account for much of the data obtained on biological systems including those that have been used to argue against diffusive transport. When observations and data are correctly interpreted, they not only fail to rule out diffusive transport, they favor it. In a two-part paper consisting of the present article (Part I) on the morphogen activities in the extracellular space and a sequel (Part II [9]) concerning the effects of endocytosis and receptor synthesis in the intracellular compartments, we report the mathematical underpinnings of the case for diffusive transport of morphogens presented in [8]. A principal result of Part II is the reduction of the boundary value problem (BVP) for the steady state behavior of the more complete formulation in the second part (designated as System C in [8]) to the same problem in the

simpler formulation of Part I (designated as System B in [8]). The eigenvalue problem in the linear stability analysis of System C is also reduced to the corresponding problem for the simpler System B (except for the decay time being determined by the smallest root of a different [9].

Here in Part I, we limit our discussion to a diffusion - reversible binding model corresponding to the kind investigated in [7] but now with the additional known biological process of receptor-mediated degradation. It will be seen that the well-established mechanism of degradation alone is sufficient for the existence of steady state concentration gradients for some range of biologically realistic parameter values. Since only results for one-dimensional formulation of such a model (System B) was discussed in [8], we will first analyzed in Section 2 this one-dimensional formulation. In particular, we will deduce the necessary and sufficient condition for the existence of a unique monotone decreasing steady state gradient and delineate how the shape of the gradient depends on a simple dimensionless combination of the biological parameters of the system. We will also show that the various steady state gradients are asymptotically stable with respect to small perturbations. Analogous formulations in two and three dimensions not previously discussed in [8] will then be developed and analyzed. Results from the 2-D and 3-D formulations will be seen to support the use of their 1-D counterpart for capturing the essential consequences of the morphogen activities.

As indicated earlier, a substantial amount of bound Dpp in gradient system is known to be located inside intracellular compartments, it could be said that a more realistic formulation that includes the effect of internalization of the morphogen-receptor complexes as well as receptor degradation and synthesis should be investigated instead of System B. Such a formulation and its consequences were in fact presented in [8] through the discussion of System C (and the relevant mathematical results to be reported in Part II). But as first reported in [8] and mentioned earlier in this introduction, the much more complicated BVP for determining the steady state behavior of System C can in fact be reduced exactly to one of the same form as the correspond problem for System B. Once the simpler problem for System B is solved herein, the results apply directly to System C if we properly interpret the relevant parameters of the problem as indicated in [8] and proved in [9]. It will be evident from the results in [9] that the process of reduction of System C to System B applies to other more complex models such as those involving non-receptors or genetic ablation of receptors in small clones of cells. Hence, for many features of morphogen gradients such as their steady state behavior, it is adequate and (because of their simplicity) preferable to work with a formulation without internalization as long as we interpret the input parameter values and the numerical output properly as indicated in [8] [9].

2. A One-Dimensional Diffusion-Reversible Binding-Degradation System

In [8], we focus on a Drosophila wing disc so that comparison can be made with both the recent measurements of [2] and [22] and the conclusions based on a "diffusion and receptor-binding" formulation considered in [1] [7] [8]. More specifically, we simplified the development of the wing imaginal disc of a Drosophila fly to a one-dimensional reaction-diffusion problem in which morphogen is introduced at the rate v at one end, the border between the *anterior* and *posterior* compartment of the disc, and absorbed at the other end, the edge of one of these compartments. Let $L(X,T)$ be the concentration of the diffusing morphogen specie (say Dpp) at time T and distance X from the source end $X = 0$, with $X_{\max}$ being the distance to the edge of the compartment. To the expression for diffusive transport provided by Fick's second law, $\partial L/\partial T = D'\partial^2 L/\partial X^2$ with D' being the diffusion coefficient, we add terms that incorporate the rate of receptor binding, $-k_{on}L(R_0 - [LR])$, and *dissociation*, $k_{off}[LR]$, with k_{on} and k_{off} being the binding rate constant and dissociation rate constant, respectively. R_0 is the total amount of receptors available which we will keep constant in System B investigated herein in contrast to being continuously synthesized and degraded in System C to be analyzed in [9].

As we noted previously, steady state gradients do not exist for a diffusion-(reversible) binding system without degradation; all receptors will eventually be occupied by the steadily accumulated concentration of morphogens.

In living tissues, molecules that bind receptors do not simply stay bound or dissociate–they internalize (endocytose) and degrade [22]; neither mechanism was considered prior to [8]. Let v taken be production rate of morphogens of the local source at $X = 0$. We allow for constitutive degradation of morphogen-receptor complexes by introducing a degradation rate term, with a rate constant k_{deg}, in the expression for the rate of change of the concentration of morphogen-receptor complexes $[LR]$. In this way, we obtain the following nonlinear reaction-diffusion system:

$$\frac{\partial L}{\partial T} = D' \frac{\partial^2 L}{\partial X^2} - k_{on} L(R_0 - [LR]) + k_{off}[LR] \qquad (0 < X < X_{\max}, T > 0) \tag{1}$$

$$\frac{\partial [LR]}{\partial T} = k_{on} L(R_0 - [LR]) - (k_{off} + k_{\deg})[LR] \qquad (0 \leq X \leq X_{\max}, T > 0) \tag{2}$$

(System C of Figure 2 in [8] provides a more refined formulation in which *endo- and exocytosis* and *degradation* are treated as two distinct processes. The first process internalizes the morphogen-receptor complexes at a certain rate with reversibility and the second allows some of the morphogen in the internalized complexes to degrade. For reasons indicated earlier in section 1, we will focus our discussion in this article to system (B) characterized by equations (1) and (2) and defer a report on system C to a subsequent article [9] though some results for system C have already been reported in [8].) At the end points, we have

$$X = 0: \quad \frac{\partial L}{\partial T} = v - k_{on} L(R_0 - [LR]) + k_{off}[LR], \quad X = X_{\max}: \quad L = 0 \quad (3)$$

for all $T > 0$. At $T = 0$, we have the homogeneous initial conditions $L = [LR] = 0$ for $0 \leq X \leq X_{\max}$.

We have considered including a flux term of the form $\eta \partial L/\partial X$ in the boundary condition (3) at $X = 0$ to regulate the influx of morphogens synthesized at a rate v there. With $k_{on} R_0 \gg k_{\deg}$ in the *Drosophila* wing disc, the contribution from such a flux term to the boundary condition is relatively small unless $\eta \gg k_{on} R_0 / k_{\deg}$ (with $\eta = \infty$ corresponding to no flux at $X = 0$). Since we expect a good flow of morphogens into posterior chamber of the wing disc (so that η is not large compared to $k_{on} R_0 / k_{\deg}$), we will limit consideration in this paper to the boundary conditions (3). This first approximation (leading term perturbation) solution should be adequate for some qualitative information and insight to the developmental process in the *Drosophila* wing disc.

To reduce the number of parameters in the problem defined by (1) - (3) and the initial conditions, we introduce the normalized quantities:

$$t = \frac{D'}{X_{\max}^2} T, \quad x = \frac{X}{X_{\max}}, \quad a = \frac{L}{R_0}, \quad b = \frac{[LR]}{R_0}, \quad v_0 = v \frac{X_{\max}^2}{D' R_0} \qquad (4)$$

$$f_0 = \frac{X_{\max}^2}{D'} k_{off}, \qquad g_0 = \frac{X_{\max}^2}{D'} k_{deg}, \qquad h_0 = \frac{X_{\max}^2}{D'} k_{on} R_0, \qquad (5)$$

to re-write the initial-boundary value problem (IBVP) for L and $[LR]$ in the following normalized form

$$\frac{\partial a}{\partial t} = \frac{\partial^2 a}{\partial x^2} - h_0 a(1-b) + f_0 b \qquad (0 < x < 1) \tag{6}$$

$$\frac{\partial b}{\partial t} = h_0 a(1-b) - (f_0 + g_0)b \qquad (0 \leq x \leq 1) \tag{7}$$

for $t > 0$ with the boundary conditions

$$x = 0: \quad \frac{\partial a}{\partial t} = v_0 - h_0 a(1-b) + f_0 b, \qquad x = 1: \quad a = 0 \tag{8}$$

for $t > 0$ and the homogeneous initial conditions

$$t = 0: \quad a = b = 0 \quad (0 \leq x \leq 1) \tag{9}$$

Our primary concern with this diffusion-reversible binding-degradation (DRBD) formulation (System B) is whether it can sustain steady state morphogen concentration gradients and how the formation and shape of the gradients depend on the biological rate parameters. For a fixed morphogen production rate and a sufficiently small degradation rate constant k_{deg}, System B should not differ in any significant way from the diffusion-reversible binding model and should not be able to sustain a morphogen-receptor concentration gradient. On the other hand, for a fixed degradation rate k_{deg}, we expect a threshold production rate v below which the system can sustain steady state solutions for a and (more importantly) b that are independent of time. We will determine this threshold in the next subsection.

2.1. Time-Independent Steady State Solution

We denote a time-independent steady state solution for $a(x,t)$ and $b(x,t)$ of (6) - (8) by $\bar{a}(x)$ and $\bar{b}(x)$. For this steady state solution, we have $\partial\bar{a}/\partial t = \partial\bar{b}/\partial t = 0$ so that these equations and boundary conditions become

$$\frac{d^2\bar{a}}{dx^2} - h_0\bar{a}(1-\bar{b}) + f_0\bar{b} = 0 \qquad (0 < x < 1) \tag{10}$$

$$h_0\bar{a}(1-\bar{b}) - (f_0+g_0)\bar{b} = 0 \qquad (0 \le x \le 1) \tag{11}$$

$$v_0 - h_0\bar{a}(0)[1-\bar{b}(0)] + f_0\bar{b}(0) = 0, \qquad \bar{a}(1) = 0 \tag{12}$$

We can use (11) to eliminate $\bar{b}$ from all other relevant equations to obtain a BVP for $\bar{a}$ alone:

$$\frac{d^2\bar{a}}{dx^2} = \frac{g_0\bar{a}}{\bar{a}+\alpha_0}, \quad \bar{a}(0) = \frac{v_0\alpha_0}{g_0 - v_0}, \quad \bar{a}(1) = 0 \tag{13}$$

with

$$\bar{b}(x) = \frac{\bar{a}(x)}{\bar{a}(x)+\alpha_0}, \qquad \alpha_0 = \frac{f_0+g_0}{h_0} = \frac{k_{off}+k_{\deg}}{k_{on}R_0} \tag{14}$$

Alternatively, we may eliminate $\bar{a}$ instead to get a BVP for $\bar{b}$ alone:

$$\frac{1}{(1-\bar{b})^3}\left[\frac{d^2\bar{b}}{dx^2}(1-\bar{b}) + 2\left(\frac{d\bar{b}}{dx}\right)^2\right] - \frac{g_0}{\alpha_0}\bar{b} = 0$$

$$\bar{b}(0) = \frac{v_0}{g_0}, \qquad \bar{b}(1) = 0 \tag{15}$$

We will have opportunities to use both of these formulations as each offers certain advantages for different purposes.

It is evident from the development above that the normalized steady state morphogen-receptor concentration $\bar{b}$ depends only on the following two parameters:

$$\psi \equiv \frac{g_0}{\alpha_0} = \frac{k_{deg}}{k_{deg} + k_{off}} \frac{X_{\max}^2}{D'} k_{on} R_0 \tag{16}$$

$$\beta \equiv \frac{v_0}{g_0} = \frac{v}{k_{deg} R_0} \tag{17}$$

On the other hand, with $\bar{a}(0) = v_0\alpha_0/(g_0 - v_0) = \bar{\beta}\alpha_0$ where $\bar{\beta} = \beta/(1-\beta)$, the normalized free morphogen concentration $\bar{a}$ also depends explicitly on the dimensionless degradation parameter g_0 in addition to β and ψ. Since the normalized morphogen-receptor concentration is constrained to lie in the unit interval so that $0 \leq \bar{b} \leq 1$, and the normalized free ligand concentration cannot be negative, we have from (15) and (13) the following necessary condition for the existence of a time-independent steady state concentration gradient for both a and b:

Lemma (2.1): $\beta < 1$ (so that $k_{\text{deg}} > v/R_0$) is a necessary condition for the existence of a time independent steady state solution.

Proof: We know already that $g_0 < v_0$ (so that $\bar{b}(0) = \beta > 1$ and $\bar{a}(0) < 0$) leads to biologically unacceptable steady state concentrations for both L and $[LR]$. If $g_0 = v_0$, then $\bar{a}(0)$ becomes unbounded at $x = 0$ in (13). Since this cannot be attained in finite time according to (7) and (8), a steady state also does not exist in this case.

Remarkably, the simple necessary condition above for the existence of a solution for the BVP (10)-(12) is also a sufficient condition for the existence

of a unique monotone decreasing solution for both $\bar{a}$ and $\bar{b}$ as we will state and prove in the following theorem:

Theorem (2.2): For $g_0 > v_0$ so that $\beta < 1$, there exist a unique pair of (time-independent) steady state solutions $\bar{a}(x)$ and $\bar{b}(x)$ for (10) -(12), both strictly decreasing in $[0,1]$.

Proof: The two equations (10) and (11) are both autonomous and can be integrated exactly. Anticipating the need for a general proof that applies to analogous theorems for two- and three-dimensional models, we will use a monotonicity argument on the formulation (13) to prove the theorem. It is easy to check that $\bar{a}_l(x) \equiv \bar{a}(1) = 0$ and $\bar{a}_u(x) \equiv \bar{a}(0) = \bar{\beta}\alpha_0$ constitute a *lower* solution and an *upper* solution of the BVP (13), respectively. By the monotonicity argument of [18] (see also[19]), there is a solution $\bar{a}(x)$ to (13) such that $0 = \bar{a}_l \leq \bar{a}(x) \leq \bar{a}_u = \bar{\beta}\alpha_0$. Consequently, $\bar{a}(x)$ is nonnegative, and, by (14), so is $\bar{b}(x)$.

To show uniqueness, suppose there are two solutions $\bar{a}_1(x)$ and $\bar{a}_2(x)$. Let $a(x) = \bar{a}_1 - \bar{a}_2$, then

$$a'' = \frac{g_0\bar{a}_1}{\bar{a}_1 + \alpha_0} - \frac{g_0\bar{a}_2}{\bar{a}_2 + \alpha_0} = \frac{g_0\alpha_0 a}{(\bar{a}_1 + \alpha_0)(\bar{a}_2 + \alpha_0)}, \qquad a(0) = a(1) = 0$$

with $(\ )' = d(\ )/dx$. Multiply both sides of the differential equation above by $a(x)$ and integrate the resulting relation over $[0,1]$ to obtain

$$\int_0^1 aa''dx = \int_0^1 \frac{g_0\alpha_0 a^2}{(\bar{a}_1 + \alpha_0)(\bar{a}_2 + \alpha_0)}dx \tag{18}$$

After integrating the left side by parts and applying the homogeneous boundary conditions for $a(x)$ we obtain

$$\int_0^1 (a')^2 dx + \int_0^1 \frac{g_0 \alpha_0 a^2}{(\bar{a}_1 + \alpha_0)(\bar{a}_2 + \alpha_0)} dx = 0 \tag{19}$$

Since $\bar{a}_1 \geq 0$ and $\bar{a}_2 \geq 0$, we must have $a(x) \equiv 0$ and hence uniqueness.

Finally we will show that $\bar{a}$ is monotone decreasing. Suppose there is a local maximum of $\bar{a}$ at an interior point x_0; then we have $\bar{a}''(x_0) \leq 0$. At the same time, we have from (13)

$$\bar{a}''(x_0) = \frac{g_0 \bar{a}(x_0)}{\bar{a}(x_0) + \alpha_0} \geq 0$$

because morphogen concentration has already been shown to be nonnegative. Together they require $\bar{a}(x_0) = 0$. Since $\bar{a}(x)$ is non-negative and $\bar{a}(x_0)$ is a maximum, we must have $\bar{a}(x) \equiv 0$ which violates the requirement that $\bar{a}(0) > 0$.

Since the ODE in (13) requires $\bar{a}(x)$ to be continuous and smooth, it also cannot have an admissible minimum $\bar{a}(x_0) = 0$ at an interior point x_0 with $\bar{a}(x) = 0$ for $x \geq x_0$ (otherwise, $\bar{a}(x) \equiv 0$ for $0 \leq x \leq x_0$ as well). Hence, $\bar{a}(x)$ must be monotone. *Given* the boundary conditions at the two ends, it must be monotone decreasing from $\beta\alpha_0/(1-\beta)$ to 0.

This completes the proof of Theorem (2.2).

2.2. Parametric Series Expansions for the Steady State Solution

We noted previously that the differential equation for $\bar{a}(x)$ (or $\bar{b}(x)$) is second order and autonomous; hence an exact solution for either is possible.

However, these exact solutions are not useful for several reasons. First, it is in the form of a quadrature that cannot be evaluated in terms of elementary or special functions. Also, the determination of an unknown parameter in the quadrature by a boundary condition requires the solution of a nonlinear equation for which any numerical solution procedure would involve a separate numerical evaluation of the quadrature at each iteration. Finally, the solution obtained in this way gives x as a function of $\bar{a}$ (or $\bar{b}$) instead of $\bar{a}(x)$ (or $\bar{b}(x)$). It would be useful to have a more informative explicit approximate solution for the steady state problem (accurate in some range of the parameter values) to help validate our numerical solution code for the general problem (both initial-boundary value problem (IBVP) for the time evolution of the concentration gradients and the steady state boundary value problem). For this reason, we will seek appropriate asymptotic approximations for the steady state solution in this section.

Recall that the steady state morphogen gradient $\bar{b}(x)$ depends only on two dimensionless parameters. The parameter $\beta = v_0/g_0$ characterizes the relative strength of the morphogen production rate and the degradation rate. A second parameter $\psi = h_0 g_0/(g_0 + f_0)$ characterizes essentially the relative strength of the morphogen-receptor binding rate and morphogen diffusion rate (see (17) and (16)). For the existence of a steady state solution, we have proved that β must be less than unity. Therefore, it would seem appropriate to seek a parametric series expansion of the steady state solution in terms of β. To obtain such a perturbation solution, we note that the

boundary condition $\bar{a}(0)$ may be written in terms of β: $\bar{a}(0) = v_0\alpha_0/(g_0 - v_0) = \beta\alpha_0/(1-\beta)$. With $A(x) = \bar{a}(x)/[\beta\alpha_0/(1-\beta)] = \bar{a}(x)/\bar{a}(0)$, the BVP for $\bar{a}$ may be rewritten as

$$\frac{d^2A}{dx^2} = \frac{\psi A}{1+\bar{\beta}A}, \qquad A(0) = 1, \quad A(1) = 0 \tag{20}$$

where $\bar{\beta} = \beta/(1-\beta)$. Note that the parameter ψ may be scaled out of the differential equation by setting

$$\zeta = \mu x, \qquad \mu^2 = \psi$$

so that

$$\frac{d^2A}{d\zeta^2} = \frac{A}{1+\bar{\beta}A}, \qquad A(\zeta = 0) = 1, \quad A(\zeta = \mu) = 0 \tag{21}$$

Thus *the effect of* $\psi > 1$ *is to steepen the gradient curve for* $\psi = 1$, and, *for* $\mu \gg 1$, *the gradient becomes a boundary layer phenomenon.* It is important to note that with proper re-scaling, the differential equation for the steady state solution depends explicitly on the dimensionless parameter $\bar{\beta}$ (and therefore β) only. As such, complications pertaining to multi-parameter asymptotic expansions do not arise in present problem.

If $\beta \ll 1$ (and $\bar{\beta} \ll 1$), we have a good first approximation $A \approx A_0(\zeta)$ with

$$\frac{\partial^2 A_0}{\partial\zeta^2} = A_0, \quad A_0(\zeta = 0) = 1, \quad A_0(\zeta = \mu) = 0 \tag{22}$$

For a moderately small β with $\bar{\beta} = \beta/(1-\beta) < 1$, we can expand the solution A in a parametric series in its only parameter $\bar{\beta} \equiv: \beta/(1-\beta)$:

$$A(\zeta;\bar{\beta}) = \Sigma_{k=0}^{\infty} A_k(\zeta)\bar{\beta}^k$$

The differential equation (21) then becomes

$$\left[1+\bar{\beta}\sum_{k=0}^{\infty}A_k\bar{\beta}^k\right]\sum_{k=0}^{\infty}\frac{d^2A_k}{d\zeta^2}\bar{\beta}^k=\sum_{k=0}^{\infty}A_k\bar{\beta}^k$$

with

$$\sum_{k=0}^{\infty}A_k(\zeta=0)\bar{\beta}^k=1,\quad \sum_{k=0}^{\infty}A_k(\zeta=\mu)\bar{\beta}^k=0$$

and with a leading term approximation determined by (22).

It is straightforward to show that the leading term solution is $A_0(\zeta)=\sinh(\mu(1-x))/\sinh\mu$. In terms of the original variables, we have the following result

Theorem (2.3): If $\bar{\beta}=\beta/(1-\beta)\ll 1$, the leading term of a formal perturbation solution of the steady state problem is given by

$$\bar{a}(x;\beta,\psi)=\alpha_0\bar{\beta}A(x;\beta,\psi)\sim\beta\alpha_0\frac{\sinh(\mu(1-x))}{\sinh\mu},\qquad \psi=\mu^2 \tag{23}$$

and

$$\bar{b}(x;\beta,\psi)\sim\beta\frac{\sinh(\mu(1-x))}{\sinh\mu} \tag{24}$$

This is the same solution as that for a system with $[LR]\ll R_0$ so that we may replace $R_0-[LR]$ by R_0. In the context of a formulation without receptor synthesis, the approximation may be interpreted as morphogen-receptor complexes being cleaved (releasing morphogens for degradation and freeing receptors for binding with newly synthesized morphogens) at a sufficiently rapid rate that receptors are far from being saturated. While such an assumption has the same effect as $\beta\ll 1$, the resulting model is

linear from the outset and the IBVP can be solved exactly without further approximation.

Note that (24) follows from (23) and (14). These simple leading term asymptotic expressions for the steady state $\bar{a}(x)$ and $\bar{b}(x)$ will be very useful later in the validation of the numerical solution for the evolution of morphogen gradients.

By computing the derivative of $\bar{b}(x)$ respect to x, we see that the slope of $\bar{b}(x)/\beta$ is of order μ near $x = 0$. When $\mu \gg 1$, a boundary layer exists adjacent to $x = 0$ with slope $O(\mu)$ while a boundary layer adjacent to $x = 1$, if exists, is considerably weaker with a slope $O(\mu/\sinh(\mu))$.

For $0 < 1 - \beta \ll 1$, we can seek a parametric series solution in powers of $1/\bar{\beta} = (1 - \beta)/\beta$. The leading term solutions for $\bar{a}$ and $\bar{b}$ are

$$\bar{a}(x;\beta,\psi) \sim \alpha_0\bar{\beta}(1-x)\{1 + O(\bar{\beta}^{-1})\}; \qquad \bar{b}(x;\beta,\psi) \sim \frac{\bar{\beta}(1-x)}{1+\bar{\beta}(1-x)} \quad (25)$$

The two leading term asymptotic solutions for $\beta \ll 1$ and $1 - \beta \ll 1$ delimit the shape of the steady state gradients for the entire range of admissible values of β.

2.3. Linear Stability for the Time-Independent Steady States

Now that the existence of a unique time-independent steady state ligand-receptor concentration gradient with all the right properties has been established, we want to know if it is stable. For a linear stability analysis, we make the usual ansatz on the solution:

$$a(x,\tau) = \bar{a}(x) + e^{-\lambda\tau}\hat{a}(x), \qquad b(x,\tau) = \bar{b}(x) + e^{-\lambda\tau}\hat{b}(x) \qquad (26)$$

where $\bar{a}$ and $\bar{b}$ are the steady state solutions and where the time independent portion of the perturbations, $\hat{a}$ and $\hat{b}$, are negligibly small compared to the steady state solution $\bar{a}$ and $\bar{b}$, respectively. After linearization, we have the following eigenvalue problem for $\hat{a}$ and $\hat{b}$:

$$-\lambda\hat{a} = \hat{a}'' - h_0(1-\bar{b})\hat{a} + (f_0 + h_0\bar{a})\hat{b} \tag{27}$$

$$-\lambda\hat{b} = h_0(1-\bar{b})\hat{a} - (f_0 + g_0 + h_0\bar{a})\hat{b} \tag{28}$$

with

$$-\lambda\hat{a}(0) = -h_0(1-\bar{b}(0))\hat{a}(0) + (f_0 + h_0\bar{a}(0))\hat{b}(0), \quad and \quad \hat{a}(1) = 0 \tag{29}$$

where a prime indicates differentiation with respect to x as before. We will show presently that the unique time-independent steady state concentration gradients are linearly stable by proving that λ is positive.

The relation (28) may be solved for $\hat{b}$ in terms of $\hat{a}$, making use of $\bar{b} = \bar{a}/(\bar{a}+\alpha_0)$ and $\alpha_0 = (f_0+g_0)/h_0$ to get:

$$\hat{b} = -\frac{h_0[1-\bar{b}(x)]}{\lambda - [h_0\bar{a}(x) + g_0 + f_0]}\,\hat{a} \tag{30}$$

$$= -\frac{h_0(g_0+f_0)}{[h_0\bar{a} + f_0 + g_0][\lambda - (h_0\bar{a} + g_0 + f_0)]}\,\hat{a} \tag{31}$$

Upon substituting (30) into (29), we obtain

$$K(\lambda)\hat{a}(0) \equiv \left[\lambda + \frac{h_0(1-\beta)^2(\lambda - g_0)}{(g_0+f_0) - (1-\beta)\lambda}\right]\,\hat{a}(0) = 0\,. \tag{32}$$

where we have made use of the expression for $\bar{a}(0)$ in (13). To determine eigenvalues, we re-write the relation (32) as

$$\kappa(\lambda)\hat{a}(0) \equiv \{(1-\beta)\lambda^2 - [f_0 + g_0 + h_0(1-\beta)^2]\lambda + h_0 g_0 (1-\beta)^2\}\hat{a}(0) = 0. \quad (33)$$

Note that the two roots of $\kappa(\lambda) = 0$ are both positive for $\beta < 1$ (which is needed to ensure the existence of a steady state solution).

Lemma (2.3): All the eigenvalues of (27), (28) and the boundary conditions (29) are real.

Proof. We use (30) to eliminate $\hat{b}$ from (27) leaving a second order differential equation for $\hat{a}$:

$$\hat{a}'' = -\left[\lambda - \frac{h_0(f_0+g_0)}{h_0\bar{a} + f_0 + g_0}\frac{\lambda - g_0}{\lambda - g_0 - f_0 - h_0\bar{a}}\right]\hat{a}\ . \quad (34)$$

Suppose λ is complex with eigenfunction $a_\lambda(x)$; then λ is not a zero of $K(\lambda) = 0$ so that we have as boundary conditions for (34)

$$\hat{a}(0) = 0, \qquad \hat{a}(1) = 0. \quad (35)$$

For this case, λ^* is also an eigenvalue with eigenfunction $a^*_\lambda(x)$ where $(\ )^*$ is the complex conjugate of $(\ )$. The bilinear relation

$$\int_0^1 [(a^*_\lambda)a'_\lambda - (a^*_\lambda)'' a_\lambda]dx = 0 \quad (36)$$

established with the help of the homogeneous boundary conditions (35) for $a_\lambda(x)$ and $a^*_\lambda(x)$ requires

$$(\lambda - \lambda^*)\int_0^1 \left\{1 + \frac{h_0(f_0+g_0)}{h_0\bar{a} + f_0 + g_0}\frac{h_0\bar{a} + f_0}{\delta(x;\lambda)\delta(x;\lambda^*)}\right\} a_\lambda(x)a^*_\lambda(x)dx = 0 \quad (37)$$

where

$$\delta(x;\lambda)\delta(x;\lambda^*) = |\delta(x;\lambda)|^2 = \lambda\lambda^* - 2p(x)\mathrm{Re}(\lambda) + [p(x)]^2$$

$$= \{\mathrm{Re}(\lambda) - p(x)\}^2 + \{\mathrm{Im}(\lambda)\}^2 > 0.$$

with $p(x) = h_0\bar{a}(x) + f_0 + g_0$. Since the integral is positive for any nontrivial $a_\lambda(x)$, we must have $\lambda - \lambda^* = 0$. Hence, λ does not have an imaginary part.

Theorem (2.3): All eigenvalues of the eigenvalue problem (27) - (29) are positive and hence the unique steady state morphogen gradients, $\bar{a}$ and $\bar{b}$, are linearly stable.

Proof. Suppose now $\lambda \leq 0$. In that case, we have $K(\lambda) \neq 0$ so that (35) applies. Let $\hat{a}(x)$ be a nontrivial solution of the homogeneous BVP (34) and (35) for the eigenvalue λ (which has been assumed to be non-positive). We now multiply (34) by $\hat{a}$ and integrate over the solution domain to get

$$\int_0^1 \left\{ \hat{a}\hat{a}'' + \left[\lambda - \frac{h_0(f_0+g_0)}{h_0\bar{a} + f_0 + g_0} \frac{\lambda - g_0}{\lambda - g_0 - f_0 - h_0\bar{a}} \right] (\hat{a})^2 \right\} dx = 0 \qquad (38)$$

After integration by parts and applying the homogeneous boundary conditions (35), we obtain

$$\lambda \int_0^1 (\hat{a})^2 dx = \int_0^1 (\hat{a}')^2 dx + \int_0^1 \left[\frac{h_0(f_0+g_0)}{h_0\bar{a} + f_0 + g_0} \frac{\lambda - g_0}{\lambda - g_0 - f_0 - h_0\bar{a}} \right] (\hat{a})^2 dx \qquad (39)$$

For a nontrivial solution of the eigenvalue problem, the right-hand side of (39) is positive which contradicts the assumption that λ is non-positive. Hence the eigenvalues of the eigenvalue problem (27)-(29) must be positive and the theorem is proved.

While knowing the eigenvalues being positive is sufficient to ensure the (linear) stability of the steady state morphogen concentration gradient, we also want to know the magnitude of the smallest eigenvalue and how it depends on the various biological parameters of the problem. These results would give us some idea of how quickly the system returns to the steady state after a small perturbation. As we will do a great deal of computing for the time evolution of the concentration of both free and bound morphogens from their initial conditions, the rate of decay obtained will also give us some idea on the rate of decay of the transient behavior and the time to steady state.

2.4. The Minimum Decay Rate of Transients

The eigenvalue problem defined by (34) and (35) is nonlinear in the eigenvalue parameter λ and, because of the spatially nonuniform steady state solution, the differential equation (34) is of variable coefficients. An exact analytic solution of this problem is not possible. While approximate solutions for $\beta << 1$ and $1-\beta << 1$ are possible by perturbation and asymptotic methods, it can be shown that slowest decay rate corresponds to the smaller root of $\kappa(\lambda) = 0$ [10] :

$$\lambda_{min} = \frac{\sigma - \sqrt{\sigma^2 - 4h_0 g_0 (1-\beta)^3}}{2(1-\beta)} \tag{40}$$

where

$$\sigma = h_0(1-\beta)^2 + g_0 + f_0 \tag{41}$$

This expression provides an estimate of the rate of approach to the steady state solution; it is not necessary to solve the Dirichlet eigenvalue problem (34) - (35) numerically. From this rate estimate, we will also be able to decide on an approximate time interval for which we should compute the evolution of morphogen gradients toward their steady state configurations. The usefulness of λ_{min} will be illustrated numerically in subsection (2.6).

2.5. Large Time Solution for $g_0 \leq v_0$

Now that we have learned considerably about the case $v_0 < g_0$, we ask what would be the solution of the IBVP if the necessary condition for a time-independent steady state is not met. While the answer may not be of particular interest from the perspective of morphogen gradients and cell signaling, it will be very useful in the validation of numerical solutions for the IBVP of time evolution of morphogen concentrations. Intuitively, we know what should happen when the morphogen production rate exceeds the rate of degradation: all receptors should be occupied eventually except near the absorbing end of the solution domain. In other words, for very large t, $b(x,t)$ should tend to unity except for a layer phenomenon near $x = 1$, similar to that exhibit by a similar system without degradation. It would be of interest to confirm quantitatively this anticipation and obtain the less obvious distribution of free morphogen concentration. More important for numerical simulation, however, is how a formulation that allows for morphogen degradation differs from the diffusion-(reversible) binding model

in the time it takes to approach a nearly uniform $b(x,t)$. How is this rate of approach modified by the degradation rate k_{deg}?

2.5.1. A Simple Diffusion Problem Before we seek a long time solution for the case $g_0 < v_0$, let us first consider very briefly a simple diffusion problem:

$$a_{s,t} = a_{s,xx}\,, \quad a_s(1,t) = 0, \quad a_{s,t}\,(0,t) = v_0, \quad a_s(x,0) = 0. \tag{42}$$

where $(\,)_{,z} = \partial(\,)/\partial z$. This IBVP is the limiting case of the problem for the normalized free morphogen concentration $a(x,t)$ for large t . After a long time, the last two terms in (6) are negligible compared to the first since a is increasing with time while b is approximately unity (except for a layer adjacent to the end point $x = 1$ within which a decreases from nearly unity to zero).

The exact solution of this IBVP can be obtained by the method of eigenfunction expansions:

$$\begin{aligned} a_s(x,t) = {} & v_0 t(1-x) + \frac{v_0}{6}(1-x)^3 \\ & + \frac{v_0}{3}\sum_{n=1}^{\infty} \frac{(-1)^n}{n\pi}\left(1 - \frac{6}{n^2\pi^2}\right) e^{-n^2\pi^2 t}\sin[n\pi(1-x)] \end{aligned} \tag{43}$$

For large values of t, we have

$$a_s(x,t) \sim v_0(1-x)\left[t + \frac{1}{6}(1-x)^2\right] \equiv a_p(x,t) \tag{44}$$

except for exponentially small terms. This limiting solution will play a major role in the large time behavior of morphogen gradient for $g_0 \le v_0$.

2.5.2. Change of Dependent Variables Since $b(x,t)$ can not exceed unity, we expect b to approach unity from below for large t except near $x = 1$ (since $a(1,t) = b(1,t) = 0$). In other words, we may write

$$b(x,t) = 1 + \hat{b}(x,t) \tag{45}$$

with $|\hat{b}(x,t)| = O(1)$ only in a narrow region near $x = 1$ and $0 < -\hat{b} \ll 1$ otherwise. Guided by the result for the previous simple diffusion problem (corresponding to the special case $h_0 = f_0 = g_0 = 0$), we take

$$a(x,t) = a_p(x,t) + \hat{a}(x,t) \tag{46}$$

where $a_p(x,t)$ is as defined in (44) From the solution for a_s in (43) , we expect also $|\hat{a}| \ll a_p$ for large t.

2.5.3. Governing PDEs for $\hat{a}$ and $\hat{b}$ Let $\delta = g_0/(g_0 + f_0) \leq 1$. Upon substituting (45) and (46) into (6) and (7) and neglecting $\hat{a}$ in $a = a_p + \hat{a}$ to get

$$\hat{a}_{,\tau} = \hat{a}_{,xx} + h_0[a_p\hat{b} + \alpha_0(1-\delta)(1+\hat{b})] \tag{47}$$

$$\hat{b}_{,\tau} = -h_0[a_p\hat{b} + \alpha_0(1+\hat{b})] \tag{48}$$

At the boundary points, we have the absorbing end condition at $x = 1$

$$\hat{a}(1,t) = 0, \tag{49}$$

and the linearized rate condition at $x = 0$

$$\hat{a}_{,\tau}(0,t) = h_0 a_p(0,t)\hat{b}(0,t) + f_0[1 + \hat{b}(0,t)]. \tag{50}$$

Note that the equation (48) is a differential equation for $\hat{b}$ alone and may be solved separately. However, before we do so, it is desirable to simplify the equations involved.

2.5.4. Leading Term Approximate Solution $b(x,t)$ for $\alpha_0 \ll 1$ For the range of biological parameter values of interest (see Table 1), we have $\alpha_0 \ll 1$. While we do not have to do so, we will, for simplicity, consider a first approximation for $\hat{b}$ by neglecting terms multiplied by α_0 in (48) With $\hat{b} = \hat{b}_0[1 + O(\alpha_0)]$,we have

$$\frac{\partial \hat{b}_0}{\partial t} = -h_0 a_p \hat{b}_0 \tag{51}$$

so that

$$\hat{b}_0(x,t) = -e^{-h_0 v_0 (1-x)[3t^2 + (1-x)^2 t]/6}, \tag{52}$$

$$b(x,t) \approx 1 - e^{-h_0 v_0 (1-x)[3t^2 + (1-x)^2 t]/6} \tag{53}$$

with the constant of integration chosen so that $\hat{b}_0(1,t) = -1$. Evidently, the approximate solution (53) for b for small α_0 satisfies the expected end conditions for large t except for terms small of higher order in t^{-1}. Recall that $b \approx 1 + \hat{b}_0$ vanishes at $x = 1$ (giving also $a(1,t) = 0$). At the other end, we have $\hat{b}_0(0,t) = 0$ except for exponentially small terms so that we have $b(0,t) = 1$ to the order of our approximation.

2.5.5. Leading Term Approximate Solution $a(x,t)$ for $\alpha_0 \ll 1$ To determine a corresponding leading term approximation for $\hat{a}$, denoted by $\hat{a}_0$, we

first omit $O(\alpha_0)$ terms in (47) to be consistent with the approximate solution for a leading term approximation for $\hat{b}$. With $\hat{a} = \hat{a}_0[1 + O(\alpha_0)] \approx \hat{a}_0$, (47) becomes

$$\frac{\partial \hat{a}_0}{\partial t} = \frac{\partial^2 \hat{a}_0}{\partial x^2} + h_0 a_p \hat{b}_0 \tag{54}$$

where a_p is given by (44) and $\hat{b}_0$ is given by (52). We will need boundary conditions for $\hat{a}_0$. The absorbing condition at $x = 1$ applies here also so that

$$\hat{a}_0(1, t) = 0. \tag{55}$$

Now, $\hat{b}$ is exponentially small away from $x = 1$; the boundary condition (50) for large t may be simplified to

$$\hat{a}_{0,\tau}(0, t) \approx f_0. \tag{56}$$

Except for higher order terms in t^{-1}, an approximate particular solution for the partial differential equation (54) and the two boundary conditions above is

$$a(x, t) \approx (v_0 + f_0)\left[(1 - x)t + \frac{1}{6}(1 - x)^3\right] + \frac{4(1 - x)}{h_0 v_0 t^3} e^{-h_0 v_0 (1-x) t^2/2} \tag{57}$$

This solution and the corresponding approximate particular solution for $b(x, t)$ in (53) satisfy all the relevant differential equations and boundary conditions up to terms of higher order in t^{-1} and α_0 (see also (59) below). They are only particular solutions since they do not satisfy the initial conditions $a(x, 0) = b(x, 0) = 0$.

Note that for large t, $a(x, t)$ has no boundary layer at $x = 1$ and a very weak layer of order $1/t^2$ compared to the leading term solution adjacent to

$x = 0$. Altogether, we have for $\alpha_0 \ll 1$, $g_0 < v_0$, and sufficiently large t the following approximate solution for a and b :

$$b(x,t) \approx 1 - e^{-h_0 v_0 (1-x) t^2/2}, \tag{58}$$

and

$$a(x,t) \approx (v_0 + f_0)(1-x)t. \tag{59}$$

These approximate solutions for large time for a and b will be useful for validating our numerical solutions of the original IBVP. It is interesting to note that to a leading order approximation, the degradation rate g_0 plays no role in the evolution of concentration gradients (58)-(59); it only affects $O(\alpha_0)$ terms, through the parameter $\alpha_0 = (f_0 + g_0)/h_0$, as well as the transient solutions.

2.6. Numerical Simulations

For accurate numerical solutions of the IBVP of the model, we discretize equations (6) and (7) with standard finite difference methods [20]. The spatial derivatives for the unknowns are approximated by the standard second-order central difference scheme. A fourth-order Adams-Moulton predict-corrector method is implemented for the temporal marching. Numerical resolution studies show that the numerical method is second-order accurate in space and fourth-order accurate in time. In addition, for $\beta < 1$, equation (13) for the steady-state solution is solved by a shooting method [6]. The corresponding steady-state solution computed through a time evolution study is compared with a direct steady-state numerical solution as well

as the asymptotic solutions of subsection 2.2 to validate both numerical simulations.

To study the implications of System B for characterizing the activities of morphogens, we use the values of the various biological parameters provided in [8]. In all calculations, we set $D' = 10^{-7}\text{cm}^2\text{sec}^{-1}$, $X_{\max} = 0.01\text{cm}$ and $k_{deg} = 2 \times 10^{-4}\,\text{sec}^{-1}$ for reasons given there. The initial conditions for all cases are $a = 0$ and $b = 0$.

Figures 1 and 2 depict *typical* evolution of the transient solution for a and b when $\beta > 1$ to confirm that there is no steady-state solution when the necessary condition for its existence is not met even when the binding rate (characterized by ψ) changes by an order of magnitude. Other biological parameters for both cases are listed as Case A and Case B in Table 1. The time interval between two successive curves is 250 seconds. One of the main feature of Figures 1 and 2 is that with the abundance of morphogens, receptors would eventually be fully occupied so that for any point in time, sufficiently long after the start of morphogen production, no receptors would be available for further binding except for a narrower and narrower region adjacent to the absorbing end $x = 1$. On the other hand, the normalized free morphogen concentration a would continue to increase without bound and distributes itself nearly linearly across the span of the wing disc. These features of a and b are as predicted by the approximate solutions for these two quantities for large t obtained in subsection 2.5.

The next three sets of figures confirm numerically the existence of a steady state concentration gradient when the necessary condition $\beta < 1$ is satisfied even when the binding rate changes two orders of magnitude. Figures 3 and 5 depict possible variations of steady state morphogen gradients when they exists. In Figure 3 the graphs of normalized receptor-bound morphogen concentration b are concave downward (convex) while in Figure 5 they are concave upward. The time interval between two successive curves is 600 seconds and 5000 seconds in Figures 3 and 5, respectively. At early time of the evolution in Figure 3, the free morphogen concentration a increases quickly up to around 4 seconds, then the dynamics slows down. A close-up of the local dynamics is shown in Figure 4.

Figure 6 depicts a biologically useful gradient, one that distributes patterning information broadly over the entire field of cells [8]. In principle, the gradient is most useful when b should resemble a straight line. The time interval between two successive curve is 600 seconds for this case. The solutions reach the 90% of the steady-states within 4 hours. Both the shape of the gradient and the time to reach the gradient fit in the vivo experimental data [2] [22]. Notice that early in the evolution shown in Figure 6, the free morphogen concentration a increases quickly up to around 200 seconds and the dynamics slows down afterwards (see Figure 4).

In biological units, the time needed for a time-dependent solution to reach the steady state with a relative error of ϵ may be approximated by

$$t_{eig}(\epsilon) \equiv -X_{\max}^2 ln(\epsilon)/\lambda_{min}/D' \quad \text{(seconds)}$$

where λ_{min} is given by (40). For $\beta << 1$ and $\alpha_0 = (f_0 + g_0)/h_0 << 1$, the leading term approximation for λ_{min} is

$$\lambda_{min} \sim \frac{h_0 g_0}{h_0 + g_0 + f_0} \tag{60}$$

We now compare this $t_{eig}(\epsilon)$ with results from direct numerical simulations. The exact values for the steady state of $\bar{a}(0)$ and $\bar{b}(0)$ are known, we obtain the times to reach the steady state solution by measuring the time when the $|\bar{a}(0) - a(0,t)|/\bar{a}(0)$ and $\left|\bar{b}(0) - a(0,t)\right|/\bar{b}(0)$ are both less than certain accuracy: ϵ. We denote this time for meeting this relative error ϵ by $t_{num}(\epsilon)$.

In Table 2, $t_{num}(\epsilon)$ and $t_{eig}(\epsilon)$ are listed for comparison. For a fixed ϵ, $t_{num}(\epsilon)$ (on the left of each column) and its corresponding t_{eig} (on the right of each column) are shown for a sequence of v, which correspond to a sequence of β. For the last row the times shown in the table are based on the eigenvalue estimates (60). All other parameters are fixed as $D' = 10^{-7}\text{cm}^2\text{sec}^{-1}$, $X_{\max} = 0.01\text{cm}$, $k_{on}R_0 = 0.01\text{sec}^{-1}$ and $k_{off} = 10^{-6}\text{sec}^{-1}$.

In general, the estimate t_{eig} and the numerically calculated t_{num} are in very good agreement for all β's as shown in the table. For example, for $\epsilon = 10^{-6}$ the difference between the t_{num} and t_{eig} ranges from 0.1% for a small $\beta = 0.25$ to 3% for $\beta = 0.75$. For larger ϵ, the differences tend to be larger. For $\epsilon = 0.01$ with $\beta = 0.75$ the difference is about 7%. The estimates t_{eig} using (60) are also in very good agreement with the numerical simulations for small β. It is interesting to notice that the percentage error in difference between $t_{eig}(\epsilon)$ and $t_{num}(\epsilon)$ is not monotonic in β.

3. The Two-Dimensional Formulation

In section 2, we undertook extensive analysis and computation for System B formulated in [8] for the morphogen gradient formation in a *Drosophila* wing disc. We did so for a number if reasons. First and foremost, our research constitutes a first effort to a quantitative approach to the study of morphogen gradients, particularly the feasibility of the mechanisms for their formation suggested in the literature. Such a first discussion should not be encumbered by avoidable technical complexities of more realistic formulations. This is possible because the results from our one-dimensional model are in fact characteristic of the various actual three-dimensional biological phenomena being investigated. The developments and analysis of the corresponding more realistic two- and three-dimensional systems in this and the next section will support this assertion. Also, the one-dimensional model was discussed first in part because the proofs and computations are simpler to perform and describe and those for the higher dimensional models (and for models that include additional observed biological processes such as internalization) are similar except possibly for technical detail. Finally, there is a close relationship between the results for the one-dimensional System B and their higher dimensional analogues with the latter reduced to the former either exactly or in some limiting situations. As such, the results pertaining to morphogen-receptor gradients obtained for the one-dimensional model should provide an adequate first insight to the actual cell signaling phenomenon in the *Drosophila* wing disc.

In this section, we will develop a more realistic two-dimensional extension of the one-dimensional system analyzed in section 2. In that section, diffusion of morphogens was allowed only in the direction perpendicular to the compartment border toward the edge of the Posterior (or Anterior) Compartment of the wing imaginal disc, designated as the X-direction. Here, we allow for additional diffusion in the dorsal-ventral direction, designated as the Y-coordinate. The span in the Y-direction, which is parallel to the compartment border, terminates in two opposite edges, $Y = \pm L_y$. In the special case where the disc and the morphogens producing line source at the compartment border both extend indefinitely so that $-\infty < Y < \infty$, it is expected that the steady state morphogen gradient is uniform in Y and is given by the solution of the one-dimensional model of the last section. In reality, the dorsal-ventral span is finite. We consider here the worst case scenario and take the two edges at $Y = \pm L_y$ to be absorbing so that $L(X, \pm L_Y) = 0$. This assumption is reasonable given that the cell population at the edge and beyond is highly dense so that there are plenty of receptors available to bind the morphogens that reach the edges. In that case, distributions of L and $[LR]$ would not be uniform in Y. Still, we expect (and will show below) that for L_y sufficiently large compared to $X_{\max}$, the steady state morphogen gradients are effectively given by the corresponding one-dimensional solutions as well except for a boundary layer adjacent to the two edges.

For a two-dimensional system with a line source of morphogens along the line $X = 0$, $-L_y < Y < L_y$, the two normalized governing differential equations for morphogen and morphogen-receptor concentration remain as given by (6) and (7) except for $\partial^2 a/\partial x^2$ (of the diffusion term) replaced by the two-dimensional Laplacian of a . With $y = Y/X_{\max}$ and $\ell \equiv L_Y/X_{\max}$, we have

$$\frac{\partial a}{\partial t} = \nabla^2 a - h_0 a(1-b) + f_0 b \qquad (0 < x < 1,\ |y| < \ell, t > 0) \tag{61}$$

$$\frac{\partial b}{\partial t} = h_0 a(1-b) - (f_0 + g_0) b \qquad (0 \le x \le 1,\ |y| \le \ell, t > 0) \tag{62}$$

where

$$\nabla^2(\ ) = \frac{\partial^2(\ )}{\partial x^2} + \frac{\partial^2(\ )}{\partial y^2} \tag{63}$$

Boundary conditions along the edges $x = 0$ and $x = 1$ remain the same as in the one-dimensional model:

$$x = 0: \quad \frac{\partial a}{\partial t} = v_0 - h_0 a(1-b) + f_0 b, \quad x = 1: \quad a = 0, \tag{64}$$

for $|y| < \ell$, $t > 0$.. In addition, we now have along the edges $y = \pm\ell$:

$$a(x, \pm\ell, t) = 0. \qquad (0 < x \le 1, t > 0) \tag{65}$$

The initial conditions remain homogeneous as in the one dimensional system:

$$t = 0: \quad a = b = 0, \qquad (0 \le x \le 1,\ |y| \le \ell) \tag{66}$$

3.1. Time-Independent Steady State Solutions

As in the one-dimensional case, we are interested in the time-independent steady state solution $\bar{a}(x,y)$ and $\bar{b}(x,y)$. Similar to the one-dimensional case, we can reduce the equations for the steady state solution to a single equation for $\bar{a}(x,y)$ in the form of (13) but with $d^2\bar{a}/dx^2$ replaced by $\nabla^2\bar{a}$. The boundary conditions along $x=0$ and $x=1$ are the same as in (13) but now for $|y|<\ell$. In addition, we have also the absorbing conditions $\bar{a}(x,\pm\ell)=0$. Considerations similar to the one-dimensional case lead again to a renormalization $A(x,y)=\bar{a}/(\bar{\beta}\alpha_0)$ where $\bar{\beta}=\beta/(1-\beta)$, and a reformulated BVP for $A(x,y)$:

$$\nabla^2 A=\frac{\psi A}{1+\bar{\beta}A},\qquad A(0,y)=1,\quad A(1,y)=A(x,\pm\ell)=0 \tag{67}$$

We note in particular that with morphogen production uniform along the line $x=0$, we have again $\bar{b}(0,y)=\beta$ and $\bar{a}(0,y)=\bar{\beta}\alpha_0$. Hence, the boundary conditions in (67) are again uniform in y.

The formulation of the BVP in terms of A(x,y) alone allows us to prove the existence and uniqueness of the steady state solution.

Theorem (3.1): $\beta<1$ is a necessary and sufficient condition for the existence and uniqueness of a steady state solution $\bar{a}(x,y)$ (and, by (14), $\bar{b}(x,y)$ as well) with $0\le\bar{a}(x,y)\le\bar{\beta}\alpha_0$ and $0\le\bar{b}(x,y)\le\beta$.

The proof is similar to that for the one-dimensional case with an application of the two-dimensional divergence theorem taking the place of

integration by parts in the one variable case.

Because of the absorbing edge conditions at $y = \pm\ell$, the monotonicity property of the one-dimensional gradient $\bar{b}$ is necessarily replaced by the less specific property of no interior maximum (or minimum):

Theorem (3.2): The maximum value of $\bar{a}(x,y)$ and $\bar{b}(x,y)$ cannot be attained at an interior point.

Proof: Suppose $\bar{a}$ attains a maximum value at an interior point (x_0, y_0). In that case, we must have $\bar{a}_{xx}(x_0,y_0) < 0$ and $\bar{a}_{yy}(x_0,y_0) < 0$. But these contradict the PDE for $\bar{a}$ which requires

$$\bar{a}_{xx} + \bar{a}_{yy} = \frac{g_0 \bar{a}}{\alpha_0 + \bar{a}} \geq 0. \tag{68}$$

3.2. Parametric Expansions for the Steady State Solution

For $0 < \bar{\beta} < 1$, we can again seek an appropriate parametric series solution for $A(x,y)$ in powers of $\bar{\beta} = \beta/(1-\beta)$. The leading term perturbation solution A_0 is determined by the BVP

$$\nabla^2 A_0 = \psi A_0, \qquad A_0(0,y) = 1, \quad A(1,y) = A(x,\pm\ell) = 0 \tag{69}$$

As before, the parameter $\psi = \mu^2$ may be scaled out of the problem. But as we shall see from the leading term perturbation solution below, it is prudent to delay this re-scaling process for the time being.

The solution of the BVP (69) can be obtained by the usual method of eigenfunction expansions. Because the end values of the morphogen concentration along $x = 0$ do not coincide with those of the eigenfunctions

(which vanish at $y = \pm\ell$), we do not have pointwise convergence of this eigenfunction expansion solution anywhere. However, it is possible to seek a solution in a different form to better exhibit the behavior of $A_0(x,y)$ for large ℓ.

For this purpose, we set

$$A_0(x,y) = A_L(x,y) + \frac{\sinh(\mu[1-x])}{\sinh(\mu)}$$

and rewrite the BVP in terms of $A_L(x,y)$:

$$\nabla^2 A_L = \mu^2 A_L, \qquad A_L(0,y) = A_L(1,y) = 0, \quad A_L(x,\pm\ell) = -\frac{\sinh(\mu[1-x])}{\sinh(\mu)}$$

An eigenfunction expansion solution for this new BVP is straightforward. We omit the detail of the solution process and simply give the following final result:

Theorem (3.3): For $\bar{\beta} \ll 1$, the leading term perturbation solution in $\bar{\beta}$ for $\bar{a}(x,y)$ (and $\bar{b}(x,y)$) is given by

$$\bar{a}(x,y) = \alpha_0\bar{\beta}A(x,y) \sim \beta\alpha_0 A_0(x,y) \sim \alpha_0\bar{b}(x,y)$$
$$= \beta\alpha_0 \left\{ \frac{\sinh(\mu[1-x])}{\sinh(\mu)} - \frac{2}{\pi}\sum_{n=1}^{\infty} \frac{\sin(n\pi x)}{n(1+\frac{\mu^2}{n^2\pi^2})} \frac{\cosh(\mu_n y)}{\cosh(\mu_n \ell)} \right\} \qquad (70)$$

with

$$\mu_n^2 = \mu^2 + n^2\pi^2. \qquad (71)$$

For all $|y| < \ell$, the series in (70) converges uniformly and absolutely for all $0 \le x \le 1$.

Away from the boundaries $y = \pm\ \ell$, we have for large ℓ

$$\frac{\cosh(\mu_n y)}{\cosh(\mu_n \ell)} \sim e^{-\mu_n \ell(1-|y|/\ell)}.$$

The following corollary is then an immediate consequence of the theorem above.

Corollary (3.4): For all $|y| < \ell$, $\bar{a}(x,y)$ and $\bar{b}(x,y)$ tend to their one-dimensional counterpart as $\ell \to \infty$:

$$\bar{a}(x,y;\beta,\psi) \sim \alpha_0 \bar{b}(x,y;\beta,\psi) \sim \alpha_0 \beta A_0(\zeta) = \frac{v_0}{\mu^2} \frac{\sinh(\mu(1-x))}{\sinh \mu} \qquad (72)$$

For large ℓ, $\bar{a}(x,y;\beta,\mu^2)$ and $\bar{b}(x,y;\beta,\mu^2)$ exhibit boundary layer behavior near the boundaries $y = \pm\ \ell$ as both concentrations must drop sharply from the function $\sinh(\mu[1-x])/\sinh(\mu)$ to zero.

At the other end of the range of admissible β values, we have for $1-\beta \ll 1$ the following BVP for the leading term perturbation solution A_0 in powers of $1-\beta$:

$$\nabla^2 A_0 = 0, \quad A_0(0,y) = 1, \quad A_0(1,y) = A_0(x,\pm l) = 0 \qquad (73)$$

with $\bar{a}(x,y;\beta,\psi) = \alpha_0 \beta A(x,y;\beta,\psi) \sim \alpha_0 \beta A_0(x,y)$ and $\psi = \mu^2 = g_0/\alpha_0$.

Theorem (3.5): For $1-\beta \ll 1$, the leading term perturbation solution in $1-\beta$ for $\bar{a}(x,y)$ may be taken in the form

$$A_0(x,y) = (1-x) - \sum_{n=1}^{\infty} \frac{1}{n} \sin(n\pi x) \frac{\cosh(n\pi y)}{\cosh(n\pi l)} \qquad (74)$$

with the Fourier series converging uniformly and absolutely for $|y| < 1$.

Similar to the $\beta \ll 1$ case, the solution for $1 - \beta \ll 1$ also exhibits a boundary layer phenomenon adjacent to the edges $y = \pm l$.

3.3. Linear Stability for the Time-Independent Steady States

Now that the existence of a unique time-independent steady state gradient for both concentrations, a and b, with no interior maximum has been established, we want to know if it is stable. We can proceed as we did in the one-dimensional case and set

$$a(x,y,t) = \bar{a}(x,y) + e^{-\lambda t}\hat{a}(x,y), \qquad b(x,y,t) = \bar{b}(x,y) + e^{-\lambda t}\hat{b}(x,y) \quad (75)$$

where $\bar{a}$ and $\bar{b}$ are the steady state solutions and where deviations from steady state are small perturbations. After linearization, we have the following eigenvalue problem:

$$-\lambda\hat{a} = \nabla^2\hat{a} - h_0(1-\bar{b})\hat{a} + (f_0 + h_0\bar{a})\hat{b} \quad (76)$$

$$-\lambda\hat{b} = h_0(1-\bar{b})\hat{a} - (f_0 + g_0 + h_0\bar{a})\hat{b} \quad (77)$$

with

$$-\lambda\hat{a}(0,y) = -h_0[1-\bar{b}(0,y)]\hat{a}(0,y) + [f_0 + h_0\bar{a}(0,y)]\hat{b}(0,y), \quad (78)$$

$$\hat{a}(1,y) = \hat{a}(x,\pm\ell) = 0, \qquad (0 < x < 1, |y| < \ell) \quad (79)$$

We will now show that the unique time-independent steady state concentration gradient for a (and therefore also b) is linearly stable by proving that λ is positive.

As in the one-dimensional case, we solve (77) for $\hat{b}$ in terms of $\hat{a}$, making use of $\bar{b} = \bar{a}/(\bar{a}+\alpha_0)$ and $\alpha_0 = (f_0+g_0)/h_0$ to get again (30) as an expression for $\hat{b}$ in terms of $\hat{a}$. Upon substituting (30) into (78), the end condition at $x = 0$, we obtain again $\kappa(\lambda)\hat{a}(0) = 0$ as in (33).

Given the same boundary condition at $x = 0$ for the two-dimensional problem. We have immediately:

Lemma (3.6): All eigenvalues of (76-78) must be real.

The proof of this lemma is similar to that for lemma(2.4), except integration by parts is replaced by an application of the two-dimensional divergence theorem, and will not be given here. With Lemma (3.6), we can proceed to obtain the following result on the linear stability of the steady state gradients:

Theorem (3.7): All eigenvalues of the eigenvalue problem (76)-(78) are positive and hence the unique steady state morphogen gradients, $\bar{a}$ and $\bar{b}$, are linearly stable.

Proof: Suppose now $\lambda \leq 0$. In that case, we have $\kappa(\lambda) \neq 0$ and therewith

$$\hat{a}(0,y) = \hat{a}(1,y) = \hat{a}(x,\pm\ell) = 0, \qquad (0 < x < 1, |y| < \ell) \tag{80}$$

Next, we use (30) to eliminate $\hat{b}$ from (76) leaving a second order ODE for $\hat{a}$:

$$\nabla^2\hat{a} = -\left[\lambda - \frac{h_0(f_0+g_0)}{h_0\bar{a}(x,y)+f_0+g_0}\frac{\lambda-g_0}{\lambda-g_0-f_0-h_0\bar{a}(x,y)}\right]\hat{a} \tag{81}$$

with (80) as boundary conditions. Because of the appearance of $\bar{a}(x,y)$, the partial differential equation (81) is of variable coefficients and does not admit

an explicit exact solution. As such, we will have to prove the positiveness of the eigenvalues by the same indirect method used in the one-dimensional case.

Let $\hat{a}(x,y)$ be a nontrivial solution of (81) and (80) for the non-positive eigenvalue λ which has been assumed to be non-positive. Multiply (81) by $\hat{a}$ and integrate over the solution domain to get

$$\int_{-\ell}^{\ell}\int_{0}^{1}\left\{\hat{a}\nabla^2\hat{a}+\left[\lambda-\frac{h_0(f_0+g_0)}{h_0\bar{a}+f_0+g_0}\frac{\lambda-g_0}{\lambda-g_0-f_0-h_0\bar{a}}\right](\hat{a})^2\right\}dxdy=0$$

Application of the two-dimensional divergence theorem and the homogeneous boundary conditions (80) transforms the integral above into

$$\lambda\int_{-\ell}^{\ell}\int_{0}^{1}(\hat{a})^2dxdy=\int_{-\ell}^{\ell}\int_{0}^{1}\left[(\hat{a}')^2+\frac{h_0(f_0+g_0)}{h_0\bar{a}+f_0+g_0}\frac{\lambda-g_0}{\lambda-g_0-f_0-h_0\bar{a}}(\hat{a})^2\right]dxdy \tag{82}$$

The right-hand side of (82) is positive for $\lambda \leq 0$; this contradicts the assumption that λ is non-positive. Hence the eigenvalues of the eigenvalue problem defined by (76) - (78) must be positive. Theorem (3.7) is thus proved.

3.4. Numerical Simulations

We solve the two-dimensional system (61) and (62) numerically using a finite difference method [20] which is second-order accurate both in space and time. To examine the accuracy of the numerical solutions, we first compare the numerical solutions with the asymptotic solutions (70) .

For the comparison in Table 3, we fix ψ and change β in order to study the dependence of the asymptotic solution on β. With $D' = 10^{-7}\text{cm}^2\text{sec}^{-1}$,

$X_{\max} = 100\mu$m and $L_y = 100\mu$m, we change β by varying v/R_0 ($\sec^{-1}$) for the following two sets of other parameters:

(i) $k_{on}R_0 = 0.01\sec^{-1}, k_{off} = 10^{-6}\sec^{-1}, k_{deg} = 2 \times 10^{-4}\sec^{-1}$ for $\psi = \mu^2 = 9.95$, and

(ii) $k_{on}R_0 = 0.05\sec^{-1}, k_{off} = 10^{-3}\sec^{-1}, k_{deg} = 10^{-3}\sec^{-1}$ for $\psi = \mu^2 = 25$.

Let a_{asym} and a_{num} denote the asymptotic and numerical solutions for the steady state $\bar{a}(x, y)$ respectively. In Table 3, the differences between the numerical solutions and asymptotic solutions decrease as β decreases. Since the asymptotic solution is only a leading term approximation in a parametric series in $\bar{\beta} = \beta/(1 - \beta)$ and the error is therefore expected to be $O(\beta)$. As shown in the table, both the maximum error and mean square error (denoted by $\| \|_\infty$ and $\| \|_2$, respectively) decrease by at least a factor of 2 as β is halved from 0.5 to 0.25 and then to 0.125 for both $\psi = 9.95$ and $\psi = 25$. Note that the maximum error shows exactly an $O(\beta)$ behavior for the larger $\psi(= 25)$.

Next we compare the two-dimensional solutions with the one-dimensional solutions. It is expected that these should be the same as l tends to ∞ except for boundary layers adjacent to $y = \pm l$. In fact, it is found through direct numerical simulations that even for $l = 1$ the difference between 1-D and 2-D solutions is very small for the biological useful gradients. Figure 7 shows one such situation, which corresponds to the Case 1 in Table 3. The top two pictures of Figure 7 are the two-dimensional steady-state solutions

while the bottom two pictures show the comparison of the 2-D solution at $y = 0$ with the 1-D solution at different times. The differences between 1-D and 2-D solutions are not noticeable in the pictures. The asymptotic behavior of 2-D solutions as $l \to \infty$ is best demonstrated for the case $l = 10$ shown in Figure 8. For this case, the solutions a and b are clearly uniform in y away from the boundary $y = \pm l$.

On the other hand, if l is reduced to $1/2$ with all other parameters fixed, there are some differences between the 1-D and 2-D solutions as shown in Figure 9, where the 2-D solutions are generally smaller than the 1-D solutions at $y = 0$. This behavior is expected as some morphogens are lost through the absorbing boundary condition along $y = \pm l$ and less morphogens are produced when l is smaller.

To give some indication how well the two-dimensional solution is approximated by the one-dimensional solution, we note

$$\frac{\cosh(\mu_n y)}{\cosh(\mu_n \ell)} \leq \frac{\cosh(\mu_1 y)}{\cosh(\mu_1 \ell)} \tag{83}$$

and therewith

$$\left| \frac{A_0(x)}{\sinh\left(\mu(1-x)\right) / \sinh \mu} - 1 \right| \leq \frac{\cosh(\mu_1 y)}{\cosh(\mu_1 \ell)} \tag{84}$$

Suppose we want to know for what values of y is the right side less than 10%. For $\mu_1 \ell \gg 1$ and $y < \ell$, we have

$$\frac{\cosh(\mu_1 y)}{\cosh(\mu_1 \ell)} \sim \exp(-\mu_1(\ell - y)) \leq 0.1 \tag{85}$$

requiring

$$\frac{y}{\ell} \leq 1 - \frac{2.3}{\mu_1 \ell}, \tag{86}$$

For the smaller of two values of $\psi(=\mu^2)$ of Table 3, we have $\mu_1 = 4.45$ (for $\psi = 9.95$) so that $y/\ell \leq 1 - 0.52/\ell$. In that case, the one dimensional solution is within 10% of the two-dimensional solution for about the middle half of the wing imaginal disc width for a disc of aspect ratio $\ell = 1$, and for about the middle three quarters of the disc width for $\ell = 2$. For the larger ψ value of 25, we have $y/\ell \leq 1 - 0.39/\ell$ for a 10% relative error. In that case, the relative error is within 10% for more than 80% of the disc away from the edges $y = \pm\ell$ for an aspect ratio of 2. Similar calculations can be performance for different relative errors and aspect ratios of the disc.

4. Three-Dimensional Formulations

In addition to diffusion in the Anterior-Posterior direction of the wing imaginal disc, designated as the X-coordinate, the two-dimensional extension of System B allows for diffusion in the dorsal-ventral direction, designated as the Y-coordinate. Having attained adequate insight to the effects of diffusion in these two directions on the formation of steady state concentration gradients, we are now ready to take the final step toward a fully three-dimensional formulation by allowing for diffusion in the apical-basal direction. We will consider the case where span of the wing imaginal disc in this third direction terminates in two opposite edges at $Z = 0, L_z$.

This stipulation seems well justified at the apical end where cells are connected by impenetrable cellular junctions. At the basal end however, we have the rather spongy basement membrane behaving as a saturable

absorber that allows some morphogens to pass through and absorbed and others to diffuse back. Hence, prescribing some other boundary condition at the basal end may also be justified. We consider first the extreme case of a saturated membrane so that the reflecting end condition applies. Ramifications of other possible end conditions and deficiencies will be discussed at the end of the section.

4.1. A Reflecting Condition at the Basal End

For a three-dimensional version of System B, the two governing differential equations for L and $[LR]$ remain as those for the corresponding two-dimensional system except for the Laplacian associated with the diffusion term is now in three variables. Let $z = Z/X_{\max}$ and $\ell_z = L_z/X_{\max}$. In terms of these dimensionless quantities and other auxiliary variables defined earlier, the two governing equations for the problem become

$$\frac{\partial a}{\partial t} = \nabla^2 a - h_0 a(1-b) + f_0 b \tag{87}$$

for $0 < x < 1, \quad |y| < \ell, \quad 0 < z < \ell_z, \quad t > 0,$

$$\frac{\partial b}{\partial t} = h_0 a(1-b) - (f_0 + g_0)b \tag{88}$$

for $0 \le x \le 1, \quad |y| \le \ell, \quad 0 \le z \le \ell_z, \quad t > 0$ where

$$\nabla^2(\ ) = \frac{\partial^2(\ )}{\partial x^2} + \frac{\partial^2(\ )}{\partial y^2} + \frac{\partial^2(\ )}{\partial z^2} \tag{89}$$

The same four boundary conditions of the two-dimensional system remain applicable so that

$$\left[\frac{\partial a}{\partial t}\right]_{x=0} = v_0 - h_0 a(0,y,z,t)[1 - b(0,y,z,t)] + f_0 b(0,y,z,t), \tag{90}$$

$$a(1, y, z, t) = a(x, \pm\ell, z, t) = 0, \qquad |y| < \ell,\ 0 < z < \ell_z,\ t > 0. \tag{91}$$

In addition, we will take as the boundary condition along the two constant Z edges the reflecting conditions

$$\left[\frac{\partial a}{\partial z}\right]_{z=0,\ell_z} = 0 \qquad (0 < x \leq 1,\ |y| < \ell,\ t > 0) \tag{92}$$

The initial conditions remain homogeneous as in the one dimensional system:

$$t = 0: \quad a = b = 0 \qquad (0 \leq x \leq 1,\ |y| \leq \ell,\ 0 \leq z \leq \ell_z) \tag{93}$$

The following theorem makes a separate treatment of this problem unnecessary:

Theorem (4.1): Any solution of the IBVP for the two-dimensional extension of System B in Section 3 (which is independent of the third variable z) is a solution of the IBVP (87) - (93).

Proof: Since a solution for the two-dimensional system does not involve the variable z, all partial derivatives with respect to z vanish. It follows that the solution for the two-dimensional problem also satisfies all the governing equations, boundary conditions and initial conditions, particularly the new reflecting boundary conditions along $z = 0, \ell_z$.

Corollary (4.2): There exists a unique steady state concentration pair $\bar{a}(x, y, z)$ and $\bar{b}(x, y, z)$ such that $0 \leq \bar{a}(x, y, z) \leq \beta\alpha_0/(1 - \beta)$ and $0 \leq \bar{b}(x, y, z) \leq \beta$. Moreover, these gradients do not attain a (local) extremum in the interior of the solution domain.

Proof: The results follow from Theorems (3.1), (3.2), and (4.1).

Corollary (4.3): If $\bar{\beta} \equiv \beta/(1-\beta) \ll 1$, a leading term perturbation solution for $\bar{a}(x,y,z)$ is given by (70) and (71). The corresponding expression for $\bar{b}(x,y,z)$ is obtained by substituting the expression (70) into (14).

Proof: The result follows immediately from theorems (3.3) and (4.1).

Corollary (4.4): The steady state solution for the three-dimensional System B is linearly stable

Proof: The result is a consequence of Theorems (3.7) and (4.1).

4.2. An Absorbing Condition at the Basal End

The stipulation of a reflecting end condition at both the apical and basal end has led to morphogen gradients uniform in the z-direction. If the absorbing basement membrane is not saturated, we should consider the other extreme case of an absorbing end condition at the basal end. We will simply state the corresponding results for this case below.

Theorem (4.5): Corollary (4.2) continues to hold for a three-dimensional extension of System B in which the reflection condition for $\bar{a}(x,y,z)$ at the basal end $z = \ell_z$ is replaced by an absorbing condition.

Theorem (4.6): If $\bar{\beta} \ll 1$, a leading term approximation for $\bar{a}(x,y,z)$ is given by

$$\bar{a}(x,y) = \bar{\beta}\alpha_0 A(x,y,z) \sim \beta\alpha_0 A_0(x,y,z) \tag{94}$$

where

$$A_0(x,y,z) = \frac{\sinh(\mu(1-y))}{\sinh\mu} - \frac{4}{\pi^2}\sum_{m=0}^{\infty}\sum_{n=l}^{\infty}\frac{(-1)^m\sin(n\pi x)}{n(1+\frac{\mu^2}{n^2\pi^2})(m+\frac{1}{2})}f_{mn}(y,z) \tag{95}$$

with

$$f_{mn}(y,z) = \frac{\cosh(\mu_{mn}y)}{\cosh(\mu_{mn}\ell)}\cos\left((m+\frac{1}{2})\frac{\pi z}{\ell_z}\right) + \frac{\cosh(\mu_{mn}z)}{\cosh(\mu_{mn}\ell_z)}\cos\left((m+\frac{1}{2})\frac{\pi y}{\ell}\right) \tag{96}$$

$$\mu_{mn}^2 = \mu^2 + n^2\pi^2 + (m+\frac{1}{2})^2\pi^2 \tag{97}$$

and a corresponding solution for $\bar{b}(x,y,z)$ is obtained from (14).

Corollary(4.7):

$$\frac{1}{\ell_z}\int_0^{\ell_z} A_0(x,y,z)dz = \frac{\sinh(\mu(1-y))}{\sinh\mu} - \frac{4}{\pi^2}\sum_{m=0}^{\infty}\sum_{n=l}^{\infty}\frac{\sin(n\pi x)}{n(1+\frac{\mu^2}{n^2\pi^2})}\bar{f}_{mn}(y) \tag{98}$$

where

$$\bar{f}_{mn}(y) = \frac{1}{\pi(m+\frac{1}{2})^2}\frac{\cosh(\mu_{mn}y)}{\cosh(\mu_{mn}\ell)} + \frac{\tanh(\mu_{mn}\ell_z)}{\ell_z\mu_{mn}(m+\frac{1}{2})}\cos\left((m+\frac{1}{2})\frac{\pi y}{\ell}\right) \tag{99}$$

We note that the apical-basal depth, L_z ($\approx$ 30 microns), is only a fraction of X_{max} with each cell spanning the full depth. Also, the distribution of receptors along the cell surface in the apical-basal direction is often nonuniform. Nonuniform receptor synthesis is included in our research on System C [9]. However, the present formulation should be adequate since what really matters to the cell development in many cases is the aggregate of $[LR]$ concentration over L_z. The result of Corollary (4.7) show that the integrated behavior of $\bar{a}(x,y,z)$ and $\bar{b}(x,y,z)$ is closer to the corresponding

results for the corresponding two-dimensional system which is in turn adequately approximated by the solution of the one-dimensional problem away from the edge $y = \pm\ell$. The coefficients $\bar{f}_{mn}(y)$ is of the order of $1/m^2$ while the coefficient multiplying $f_{mn}(y,z)$ is only $O(1/m)$. Still, the concentration gradients for the case of an absorbing basement membrane is different from those for a reflecting condition at both ends. With one absorbing end, there would be less morphogens and the available morphogens would be distributed nonuniformly across L_z . The effect of other possible boundary conditions appropriate for the saturable basement membrane are likely to fall between those for a reflecting conditions and an absorbing condition for the basal end.

For some biological setup, nonuniformity in the apical-basal (z-) direction may also be induced by a morphogen source at the end $x = 0$ that is nonuniform in z. In some cases, the source may be localized around the line y = 0. In these cases, the solution to the three-dimensional problem would also not be uniform in z, and a more elaborate (but manageable) analysis would be needed for the problem. We do not know whether or not this is the situation in the wing imaginal disc of the Drosophila flies, but each cell is a pseudostratified epithelium that spans the full length L_z. It probably does not matter whether [LR] varies with z near the morphogen source (x = 0). Again, only the effect of the aggregate concentration along the z-direction is likely to matter to any one cell.

5. Conclusion

In section 2 of the developments above, we provided the mathematical results that underpin the conclusions reached in [8] for System B formulated there to study the effects of diffusion (in the anterior-posterior direction), reversible receptor-morphogen binding, and degradation. The principal results consist of establishing the existence of a unique, linearly stable steady state morphogen-receptor concentration gradient with all the right properties under biologically meaningful conditions. A simpler system without degradation is known not to have the desired steady state gradient and we may reach a similar (but incorrect) conclusion for a formulation that includes degradation such as System B if we had computed with the wrong range of parameter values for which steady state gradients are now known from lemma 2.1 not to exist. At the same time, it is rather remarkable to have from Theorem 2.2 (and its higher dimension analogues) that the existence of a unique steady state for the various concentration gradients depends only on a single dimensionless parameters, β, corresponding to the ratio of the morphogen production rate (per unit receptor) and the morphogen-receptor complex degradation rate (not on other parameters such as dissociation rate). A second dimensionless parameter ψ corresponding to the ratio of binding rate and the loss rate of $[LR]$, determines the shape (and hence the usefulness) of the $[LR]$ gradient. A more realistic two-dimensional formulation that allows for diffusion in the ventral-dorsal direction was developed and analyzed in section 3. For that formulation,

the results obtained reduce to those of the corresponding one-dimensional System B either exactly or in some limiting cases. A three-dimensional version of System B that allows for diffusion in the apical-basal direction as well is developed and analyzed in section 4. Stipulating a reflecting condition at the apical and basal end made it possible to conclude that the solution of the corresponding two-dimensional system applies directly without modification. The case of an absorbing basal end was also analyzed to provide two extreme scenarios to bracket intermediate spongy basal end condition.

While it is gratifying to see that steady state concentration gradients can exist under biologically realistic condition, a more important question is whether these gradients are biologically useful. For them to be useful in specifying a pattern across the wing disc, the morphogen-receptor distribution in the wing imaginal disc compartment should be neither in the form of a boundary layer adjacent to the source end nor spreading uniformly over the disc span. This issue of useful gradients was investigated in [8] with the finding that the resulting steady state gradients are in fact useful in some range of biologically realistic parameter values but not in others. At the same time, additional biological processes such as morphogen binding to molecules other than receptors, internalization, receptor degradation and synthesis, feedback mechanism, etc. may have adverse effects on the positive findings and will need to be investigated.

Still the benefits of investigating the simpler model B are much more than the results mentioned above. It was already reported in [8] that the

problem of steady state gradients for System C, an extension of system B to allow for receptor degradation and synthesis, endocytosis and exocytosis of morphogen-receptor complexes, can be shown to be formally identical to that in section 2 for System B. Hence the results obtained for the simpler problem here are directly applicable to the more realistic System C. It will be evident from the results in [9] that the process of reduction of the steady state aspects of System C to those of System B applies to other more complex systems such as one involving non-receptors or genetic ablation of receptors in small clones of cells. Hence, for many features of morphogen gradients of these more complex models (such as their steady state behavior), it is adequate and preferable (because of their simplicity) to work with formulations without internalization as long as we interpret the input parameter values and the numerical output properly.

References

1. Crick, F.H.C., "Diffusion in embryogenesis," Nature, Vol. 225, 1970, 40-42.
2. Entchev, E.V., Schwabedissen, A. and Gonzalez-Gaitan, M., "Gradient formation of the TGF-β Homolog Dpp", Cell, Vol. 103, 2000, 981-991.
3. Gonzalez, F., Swales, L., Bejsovec, A., Skaer, H., and Martinez Arias, A., "Secretion and movement of wingless protein in the epidermis of *Drosophila* embryo". Mech. Dev., Vol 35, 43-54, 1991.
4. Gonzalez-Gaitan, M., and Jackle, H., "The range of spaltactivating Dpp signalling is reduced in endocytosis- decfective *Drosophila* wing discs." Mech. Dev. Vol 87, 143-151, 1999.
5. Gurdon, J.B., and Bourillot, P.Y., "Morphogen gradient interpretation, Nature, Vol. 413, 2001, 797-803.

6. Keller, H.B., *Numerical Methods for Two-Point Boundary Value Problems*, Dover Publications, New York, 1992.

7. Kerszberg, M. and Wolpert, L., Mechanisms for positional signaling by morphogen transport: a theoretical study," J. Theor. Biol., Vol. 191, 1998, 103-114.

8. Lander, A.D., Nie, Q. and Wan, F.Y.M., "Do Morphogen Gradients Arise by Diffusion?" Developmental Cell, Vol. 2, 2002, 785-796.

9. Lander, A.D., Nie, Q. and Wan, F.Y.M., "Diffusion and Morphogen Gradients–Part II: The Effects of Endocytosis and Receptor Synthesis", submitted, 2003

10. Lou, Y., Nie, Q. and Wan, F.Y.M., "Some Nonlinear Eigenvalue Problems Related to Stability of Morphogen Gradients" to appear, 2003

11. Maini, P.K., and Othmer, H.G., *Mathematical Models for Biological Pattern Formation*, Springer, New York, 2001.

12. Meinhardt, H, "On pattern and growth". In M.A.J. Chaplain, G. D. Singh, and J.C. McLachlan, editors, *Spatio-Temporal Pattern Formation in Biology*, pages 129-148. John Wiley, New York, 1999

13. Monk, N.A.M., "Restricted-range Gradients and Traveling Fronts in a Model of Juxtacrine Cell Relay," Bulletin Math. Biol., Vol.60, 1998, 901-918.

14. Murray, J.D., *Mathematical Biology*, 3rd ed., Springer-Verlag, New York, 2003

15. Plahte, E., "Pattern formation in discrete cell lattices," J. Math. Biol., Vol. 43, 2001, 411-445.

16. Page, K.M., Maini, P.K., Monk, N.A.M., and Stern, C.D., "A Model of Primitive Streak Initiation in the Chick Embryo," J. Theor. Biol., Vol. 208, 2001, 419-438.

17. Satnoianu, R.A., Menzinger, M., Maini, P.K., "Turing instability in general systems," J. Math. Biol., Vol. 41, 2000, 493-512.

18. Sattinger, D.H., "Monotone Methods in Nonlinear Elliptic and Parabolic Boundary Value Problems," Indiana University Math. J., Vol. 21, 1972, 981-1000.

19. Smoller, J., *Shock waves and reaction-diffusion equations*, Springer Verlag New York Inc., 1982.

20. Strikwerda, J.C., *Finite Difference Schemes and Partial Differential Equations*, Wadsworth & Brooks/Cole. Pacific Grove, CA, 1990

21. Tabata, T., and Komberg, T.B. "Hedgehog is a signaling protein with a key rol in patterning *Drosophila* imaginal discs", Cell, Vol 76, 89-102, 1994.

22. Teleman, A.A., and Cohen, S.M., "Dpp gradient formation in the Drosophila wing imaginal disc," Cell, Vol. 103, 2000, 971-980

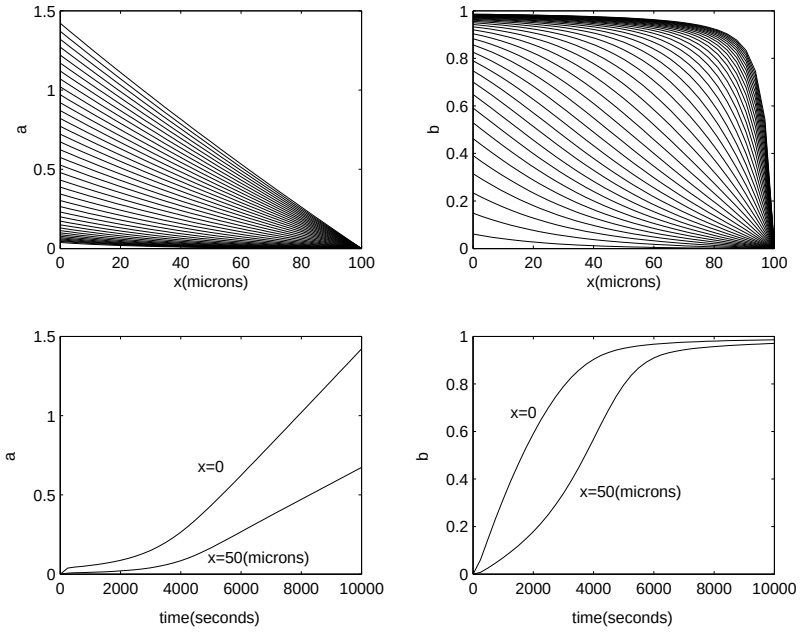

Fig. 1. Dynamics of the gradient. Parameters are those for Case A of Table 1: $\beta = 2.0, \psi = 10.0$. There is no steady-state; the evolution toward receptor saturation is slow.

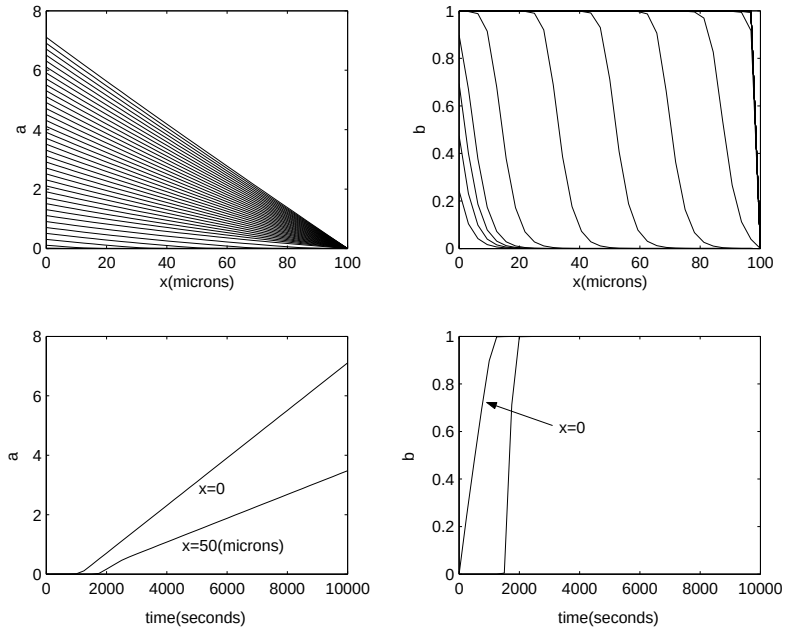

Fig. 2. Dynamics of the gradient. Parameters are those for Case B of Table 1: $\beta = 5.0, \psi = 995$. Evolution toward receptor saturation is much faster than case A. There is no steady-state for this case.

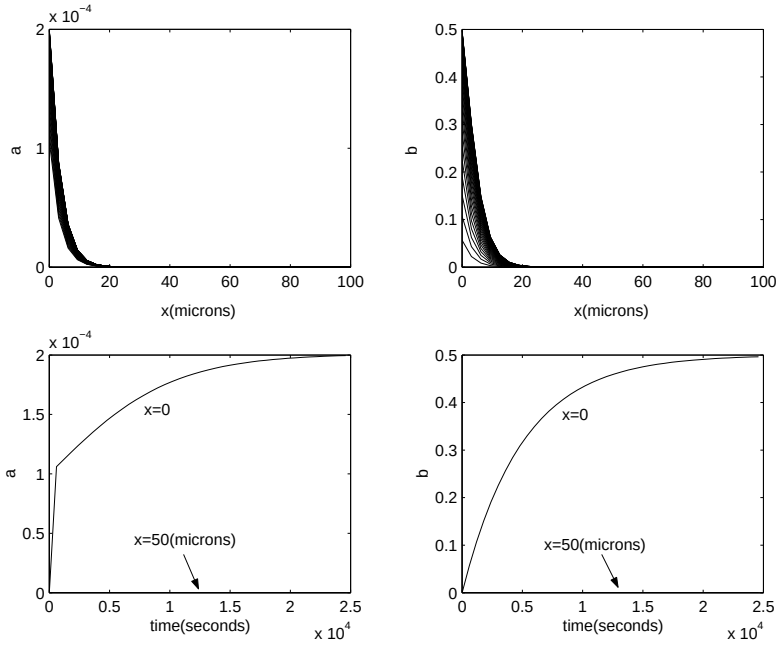

Fig. 3. Dynamics of the gradient. Parameters are those in Case C of Table 1: $\beta = 0.5, \psi = 995$. A steady state gradient exists but is not biologically useful.

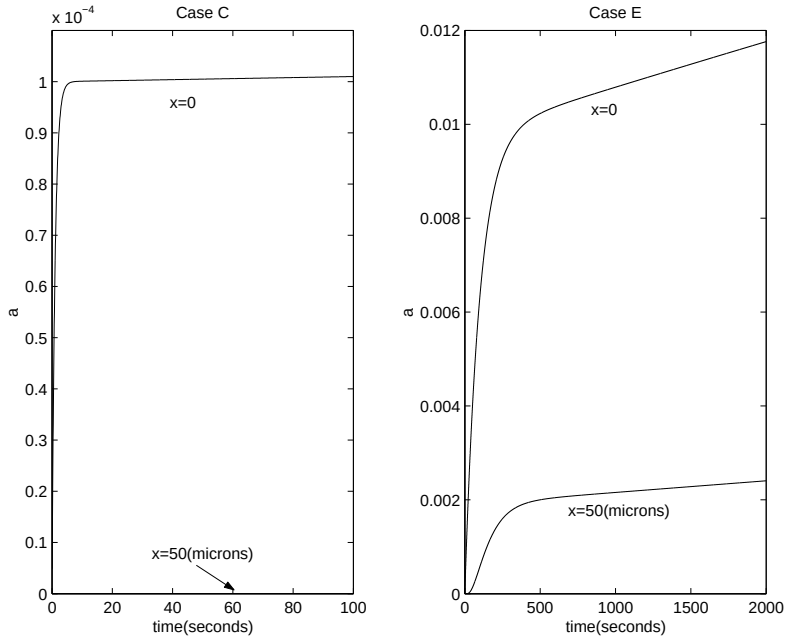

Fig. 4. Early time dynamics of free morphogen concentration of $a = L/R_0$ at the location of $X = 50 microns$ and $X = 0$ for case C and Case E in Table 1. Approach to steady state is much slower in Case E

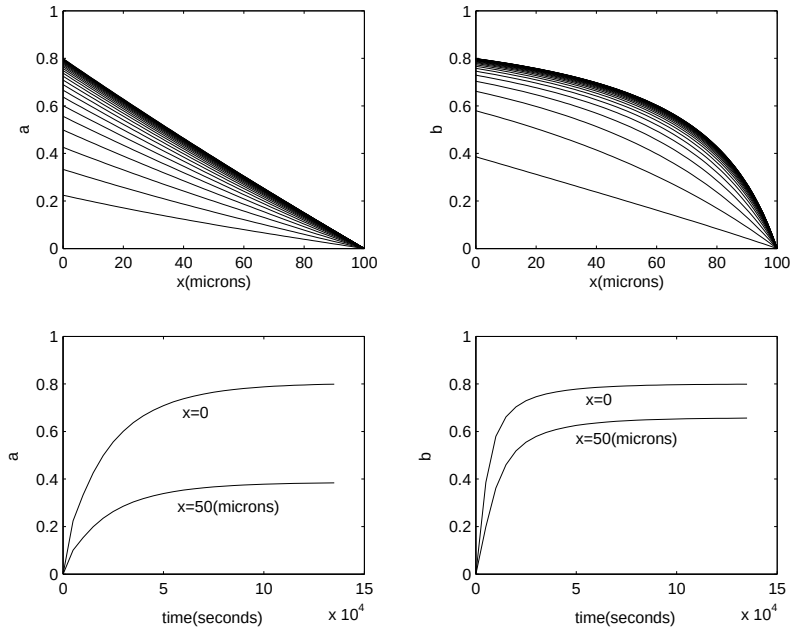

Fig. 5. Dynamics of the gradient. Parameters as in Case D of Table 1: $\beta = 0.8, \psi = 1.0$. Approach to steady state is much faster here than in Case C and E though the v to k_{deg} ratio is larger.

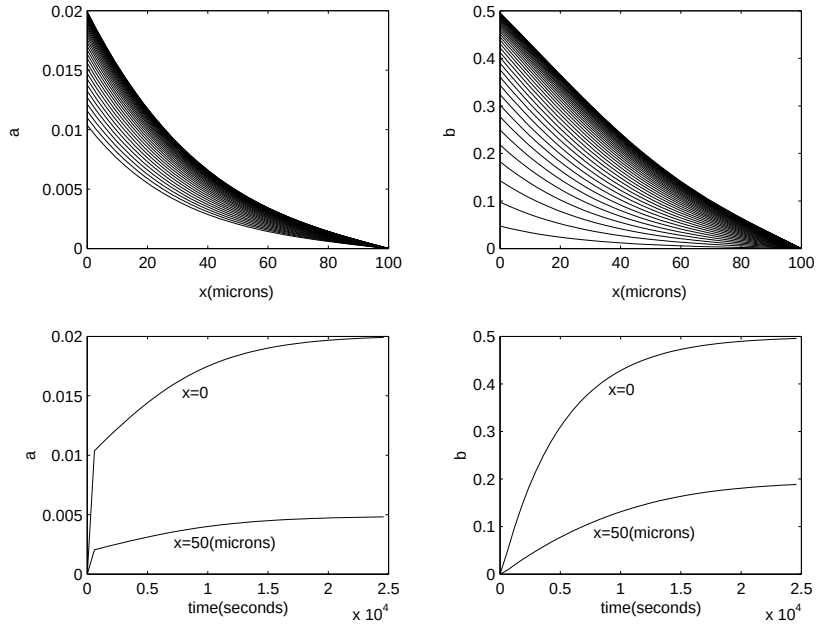

Fig. 6. Dynamics of the gradient. Parameters as in Case E of Table 1: $\beta = 0.5, \psi =$ 10. The gradient is close to linear and biologically useful for tissue patterning.

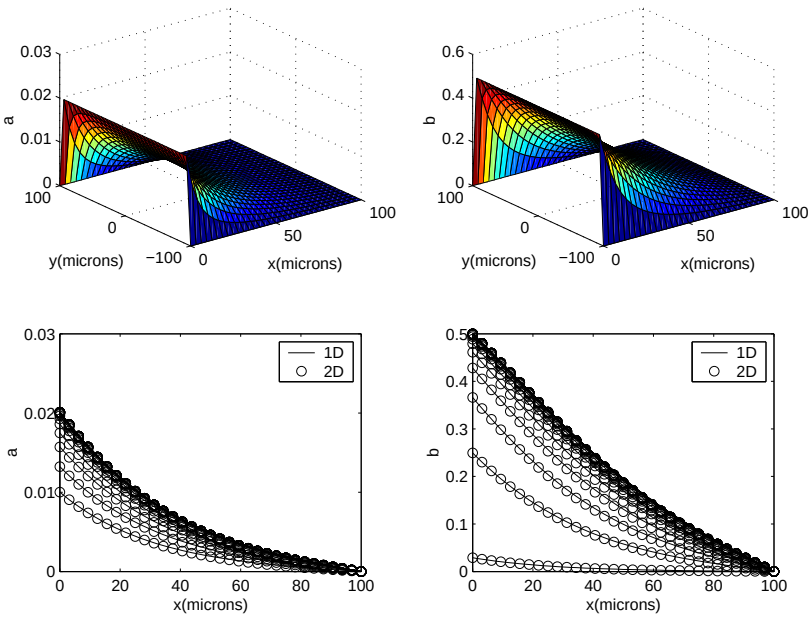

Fig. 7. Comparison between the 1-D and 2-D solutions. The starting curve is at 800 seconds, the time interval between two successive curves is 3200 seconds

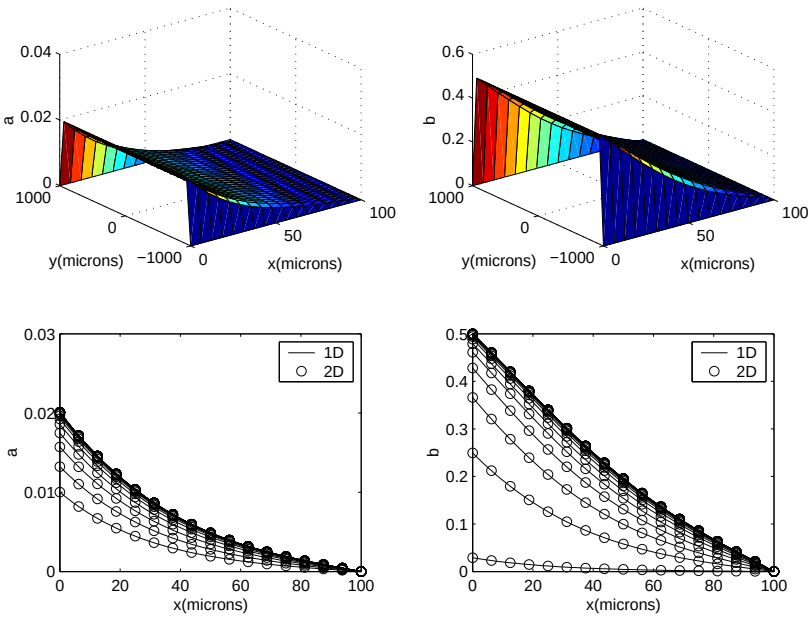

Fig. 8. Comparison between the 1-D and 2-D solutions. The starting curve is at 800 seconds, the time interval between two successive curves is 3200 seconds

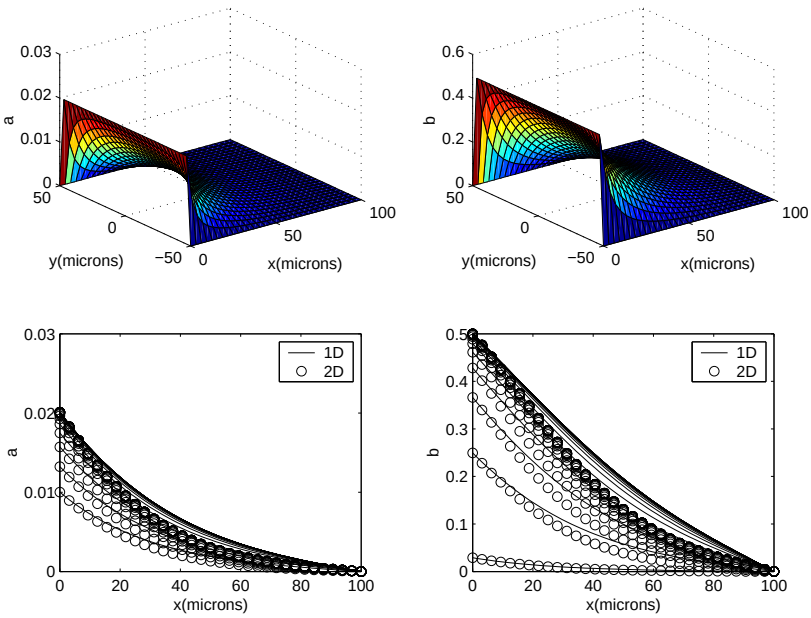

Fig. 9. Comparison between the 1-D and 2-D solutions. The starting curve is at 800 seconds, the time interval between two successive curves is 3200 seconds

Case	$v0/R_0$	$k_{on}R_{tot}$	k_{off}	β	ψ
A	4×10^{-4}	0.01	10^{-6}	2.0	10.0
B	10^{-3}	1.0	10^{-6}	5.0	995
C	10^{-4}	1.	10^{-6}	0.5	995
D	1.6×10^{-4}	10^{-3}	10^{-6}	0.8	1.
E	10^{-4}	0.01	10^{-6}	0.5	10.0

Table 1. List of parameters for calculations. β and ψ have no units and other parameters are in units of $\sec^{-1}$

	$\epsilon = 10^{-2}$	$\epsilon = 10^{-3}$	$\epsilon = 10^{-6}$
v_0/R_0 (β)	t_{num}, t_{eig}	t_{num}, t_{eig}	t_{num}, t_{eig}
1.8×10^{-4} (0.9)	69500, 67743	103300, 101613	204900, 203228
1.5×10^{-4} (0.75)	26300, 28167	40700, 43450	84100, 86900
10^{-4} (0.5)	11900, 11997	35800, 35990	71800, 71980
5×10^{-5} (0.25)	23300, 23240	34900, 34860	69800, 69721
2×10^{-5} (0.1)	23200, 23087	34700, 34630	69400, 69261
λ_{min} in (60)	23028	34542	69085

Table 2. Comparison on the times to reach the steady-states between the numerical transient solutions and the linearized eigenvalue solution

Case	v_0/R_0	β	ψ	$\|a_{num} - a_{asym}\|_\infty$	$\|a_{num} - a_{asym}\|_2$
1	10^{-4}	0.5	9.95	1.70×10^{-2}	1.0×10^{-4}
2	5×10^{-5}	0.25	9.95	5.58×10^{-3}	3.14×10^{-5}
3	2.5×10^{-5}	0.125	9.95	2.51×10^{-3}	1.31×10^{-5}
4	2.5×10^{-4}	0.25	25	1.0×10^{-2}	5.03×10^{-5}
5	1.25×10^{-4}	0.125	25	5.0×10^{-3}	2.08×10^{-5}
6	6.25×10^{-5}	0.0625	25	2.50×10^{-3}	9.63×10^{-6}

Table 3. Comparison between the numerical solutions and asymptotic solutions